



Review

A Global Systematic Review of Improving Crop Model Estimations by Assimilating Remote Sensing Data: Implications for Small-Scale Agricultural Systems

Luleka Dlamini ^{1,2,*} , Olivier Crespo ¹ , Jos van Dam ² and Lammert Kooistra ³

¹ Climate System Analysis Group, University of Cape Town, Cape Town 7700, South Africa

² Soil Physics and Land Management Group, Wageningen University & Research, 6708 PB Wageningen, The Netherlands

³ Laboratory of Geo-Information Science and Remote Sensing, Wageningen University & Research, 6708 PB Wageningen, The Netherlands

* Correspondence: dlmlul001@myuct.ac.za

Abstract: There is a growing effort to use access to remote sensing data (RS) in conjunction with crop model simulation capability to improve the accuracy of crop growth and yield estimates. This is critical for sustainable agricultural management and food security, especially in farming communities with limited resources and data. Therefore, the objective of this study was to provide a systematic review of research on data assimilation and summarize how its application varies by country, crop, and farming systems. In addition, we highlight the implications of using process-based crop models (PBCMs) and data assimilation in small-scale farming systems. Using a strict search term, we searched the Scopus and Web of Science databases and found 497 potential publications. After screening for relevance using predefined inclusion and exclusion criteria, 123 publications were included in the final review. Our results show increasing global interest in RS data assimilation approaches; however, 81% of the studies were from countries with relatively high levels of agricultural production, technology, and innovation. There is increasing development of crop models, availability of RS data sources, and characterization of crop parameters assimilated into PBCMs. Most studies used recalibration or updating methods to mainly incorporate remotely sensed leaf area index from MODIS or Landsat into the World Food Studies (WOFOST) model to improve yield estimates for staple crops in large-scale and irrigated farming systems. However, these methods cannot compensate for the uncertainties in RS data and crop models. We concluded that further research on data assimilation using newly available high-resolution RS datasets, such as Sentinel-2, should be conducted to significantly improve simulations of rare crops and small-scale rainfed farming systems. This is critical for informing local crop management decisions to improve policy and food security assessments.

Keywords: process-based crop models; earth observation; data assimilation; crop yield estimates; data limitation



Citation: Dlamini, L.; Crespo, O.; van Dam, J.; Kooistra, L. A Global Systematic Review of Improving Crop Model Estimations by Assimilating Remote Sensing Data: Implications for Small-Scale Agricultural Systems. *Remote Sens.* **2023**, *15*, 4066. <https://doi.org/10.3390/rs15164066>

Academic Editors: Jianxi Huang and Mario Cunha

Received: 1 June 2023

Revised: 2 August 2023

Accepted: 12 August 2023

Published: 17 August 2023



Copyright: © 2023 by the authors. Licensee MDPI, Basel, Switzerland. This article is an open access article distributed under the terms and conditions of the Creative Commons Attribution (CC BY) license (<https://creativecommons.org/licenses/by/4.0/>).

1. Introduction

Global agricultural systems are under significant pressure due to population growth, limited productive land, water scarcity, and climate change. In Africa, these pressures further exacerbate in small-scale farming systems that are highly dependent on erratic rainfall and affected by various socioeconomic factors, such as poverty, food insecurity, and limited access to technical support and financial resources, which limit their ability to adapt to multiple stressors [1,2]. Therefore, there is a need to find agricultural land management strategies that maximize food production with lower resource inputs, often referred to as “sustainable intensification” [3], especially in small-scale farming systems.

Process-based crop models (PBCMs) are among the essential numerical tools used to explore the effects of potential sustainable agricultural land management practices on crop

growth and yield [4,5]. Such models use mathematical equations to capture the relationship between a crop's environmental conditions and mechanistic biophysical processes [6]. In addition, they focus on dynamically describing the physiological processes that drive plant growth, including photosynthesis, respiration, and evapotranspiration [7]. Thus, PBCMs can estimate potential or water-limited yield as a function of climate, soil conditions, and cropping practices. At the same time, they simulate crop growth limits at the model's time step (i.e., daily). PBCMs can be used as a decision-support tool to evaluate the effects of current and future limiting factors, such as climate, soil, water, nutrient stress, and crop management, on crop growth and yield. However, numerous uncertainties often compromise the performance of these models, particularly the quality and quantity of input data required to initialize and calibrate PBCMs [8,9]. For example, applying PBCMs for estimating crop growth and yield over large areas remains limited due to the lack of essential information on spatial variations in soil properties, weather variables, crop varieties, plant conditions variables, and crop management strategies [10]. Additional uncertainties may arise from model parameterization (e.g., exclusion of diseases and pest effects), climate drivers (e.g., localized frost), and simplified model process descriptions. These uncertainties reduce the accuracy with which the models can be used to estimate crop growth and yield, limiting the utility of their applicability.

Several studies have proposed integrating external observations of crop parameters from remote sensing (RS) into crop models to improve model calibration and the accuracy of estimates, a process called data assimilation [11,12]. Data assimilation can be used when there are uncertainties in certain model input values. In addition, it can be used to adjust the model to account for excluded biophysical processes to reduce discrepancies between model estimates and actual observations. The continuous development of RS technology and sensors has led to a timely, accurate, and consistent collection of estimates for certain key biophysical variables of crops at field and regional scales [13,14]. Accessible and inexpensive datasets from RS can be used to measure several plant variables, including the leaf area index (LAI) [12], soil moisture (SM) [15], evapotranspiration (ET) [16], nitrogen content [17], chlorophyll content [18], and the fraction of absorbed photosynthetically active radiation (FAPAR) [19]. The inclusion of these variables in the PBCMs leads to a better characterization of the heterogeneity within the agricultural systems and a reflection of actual seasonal vegetation dynamics in the simulations.

There are increasing efforts to use the dynamic simulation capacity of PBCMs in conjunction with access and spatial quantification of RS data. Currently, three data assimilation methods are used to assimilate RS data into a PBCM: forcing, recalibration, and updating. In the forcing method, the state variables in the crop model are replaced with estimated RS data to improve the simulation results [20]. In the recalibration method, the state variables are re-initialized or re-estimated to an optimal level using optimization algorithms that minimize the difference between the derived and model-simulated state variables [21]. The updating method assumes that better estimation of the model state variables on "day *t*" by combining model estimation and RS observation will increase the accuracy of the model-simulated variables over subsequent days [22]. Therefore, model state variables are updated directly as observed RS data become available. A typical data assimilation process and the differences between data assimilation methods are best illustrated in previous reviews [23,24]. Nevertheless, the extent to which these methods have been applied worldwide and under different agricultural systems, including heterogeneous small-scale, rainfed, and often data-poor conditions, is still limited.

Several previous studies have highlighted opportunities to improve crop model estimates by assimilating RS data, including recent reviews [23–26] that focused on providing an overview of crop model development, RS technology, data assimilation methods, algorithms, and sources of uncertainty. However, none of these reviews focused exclusively on how the application of data assimilation differs by country, crop, and farming system. More specifically, none focused on how small-scale farming systems in data-limited areas such as Africa can benefit from this approach. Assessing the field's current state will also

highlight developments that will support future research and democratize the use of crop models, especially in areas with limited data. Thus, this study aims to provide a systematic overview of data assimilation research and to summarize how its application varies by country, crop, and farming system. The specific objectives are (1) to present the temporal scope and geographical distribution of relevant studies around the world; (2) to provide an overview of the major crop, crop model, and remote sensing datasets used during the data assimilation process; (3) to summarize the different data assimilation methods used and discuss their strengths and drawbacks; (4) to evaluate the agricultural systems under which these studies are conducted and discuss the challenges associated them; and (5) to highlight the implications of implementing PBCMs and data assimilation in small-scale agricultural systems.

2. Materials and Methods

2.1. Systematic Review

This study conducted a systematic literature review to adequately structure and thoroughly evaluate existing research on integrating RS data into crop models. We particularly considered the guidelines for systematic reviews in environmental management [27,28] in this study. The overarching research question, “To what extent does research focused on integrating RS data into PBCM to improve crop growth and yield estimation differ by country, crop, and farming systems?” was divided into clearly searchable concepts using the PICO framework: population; intervention; comparison; and outcome. In the present study, the PICO was defined as population—cropping systems worldwide; intervention—integration of RS data into PBCMs; comparison—data assimilation methods and algorithms; and outcome—improving crop growth and yield estimation.

2.2. Literature Selection Process

As part of this study, we conducted a broad literature search using two peer-reviewed databases of professional publications: Web of Science (Core Collection) and Scopus. These databases contain extensive, best-recorded, up-to-date, and interdisciplinary academic journals and reports [28,29]. Nevertheless, this study may have missed other relevant studies not indexed in these databases. The initial literature search included publications from 1995 to 2021, but 84% were between 2011 and 2021. Only publications published between 1 January 2011 and 31 July 2021 were considered for further analysis. We performed the database searches in English and used an asterisk (*) to capture multiple word endings, e.g., remote* to pick up both remotely and remote. We used the following general terms in the search for relevant articles were:

(remote* OR “earth observation*” OR “spatio-temporal*” OR satellite*) AND (assimilation OR “data assimilation*” OR “data integration*”) AND (“crop model*” OR “crop growth*” OR “crop simulation model*”) AND (agricultur* OR yield* OR crop* OR “vegetation indices”)

The process was iterative and allowed the exploration of different keywords. We used rigorous inclusion/exclusion criteria to select relevant articles that addressed improving crop model estimates by assimilating remote sensing data. Table 1 and Figure 1 summarize the data selection process.

Table 1. The inclusion and exclusion criteria for the literature selection.

Search Protocol	Inclusion Criteria	Exclusion Criteria
Initial database and document search	English literature	Non-English literature
	The use of both remote sensing and crop models	Studies on the exclusive use of remote sensing or crop models
	Application in cropping systems	Application in other sectors such as hydrology, health, fire, forests, and pests

Table 1. *Cont.*

Search Protocol	Inclusion Criteria	Exclusion Criteria
Removal of duplicates	Single studies	Duplicated studies from the different databases
Title and abstract screening	Studies after 2011 Original studies Assimilation of remote sensing data into crop models to assess and/or monitor crop growth and crop yield	Studies before 2011 A literature review or discourse analysis Title and/or abstract that is out of the general scope of the current study, abstract not available, or abstract without the data assimilation of remote sensing and crop models
Full-text screening and reviewing	Assimilation of remote sensing data into crop models using forcing, recalibration, or updating methods Studies aimed at improving crop yield and the accuracy of crop growth outputs predictions Studies that used process-based crop models (PBCMs) Clearly stated the assimilation algorithm used National, subnational, and local scale	No mention of data assimilation methods; remote sensing data used as a proxy indicator Studies not aimed at improving crop productivity and the accuracy of crop growth output predictions Studies that used other types of crop models No mention of the assimilation algorithm used Regional and global analyses

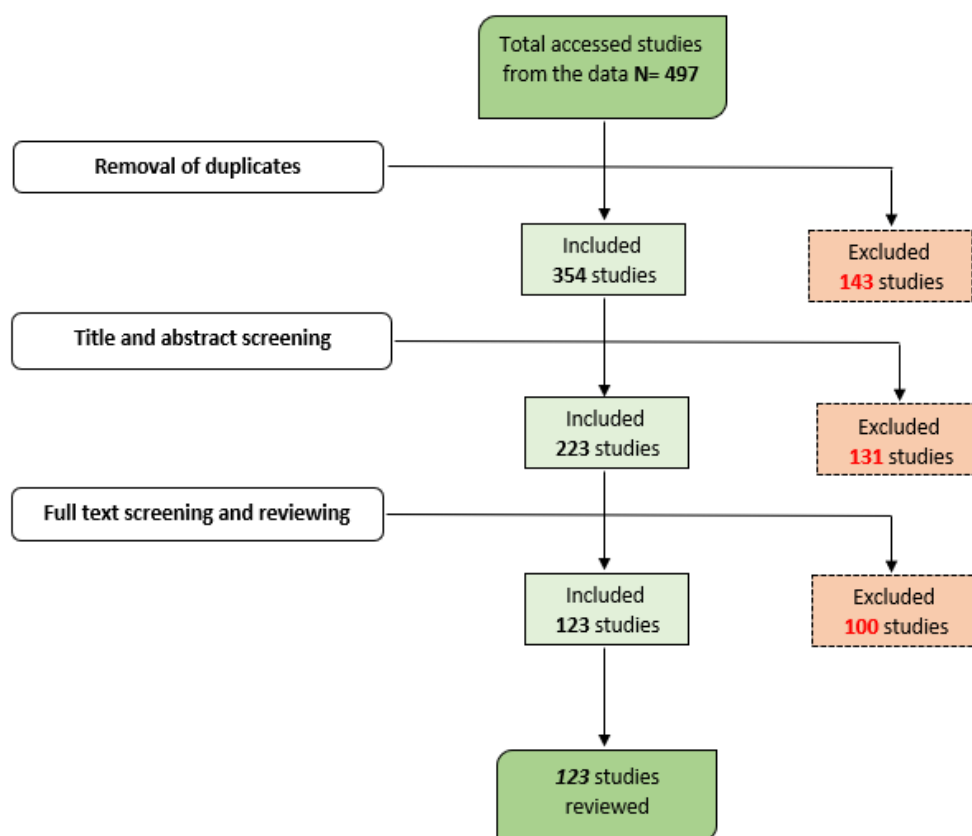


Figure 1. Summary of the literature screening process.

We imported the search results into the EndNote (<https://endnote.com/>) reference manager software for further analysis and identified 497 studies in the two databases (Figure 1). These were peer-reviewed articles and grey literature (e.g., conference proceedings, working papers, and project reports). The first screening stage consisted of automatic (using the duplicate function in EndNote) and manual removal of all duplicate publications. During the title and abstract screening, we removed all publications unrelated to this study’s objectives. In addition, we removed literature reviews and discourse studies. Only

studies that used PBCMs were included in the full-text review and rescreening, as they can evaluate multiple growth and yield limiting factors at different spatial and temporal resolutions. In addition, only studies that had full English text clearly stating the data assimilation method and algorithm used that were conducted at the national, subnational, and local levels were included in the final review. Ultimately, this systematic review consisted of 123 studies (Figure 1). These included 103 scientific journal articles (84%) and 20 conference papers (16%).

2.3. Review Analysis

The selected studies were coded for information and classified into thematic groups. These included the geographic location of the study, the crop and crop model used, the RS data used, the state variable derived from RS data, the data assimilation method and the algorithm used, the scope and overall objective of the study, the cropping system (i.e., small-scale, rainfed), and the challenges of in assimilating RS with crop models. This study defines small-scale agricultural systems as cropping systems where the main production is for subsistence and only a small portion (i.e., when there is a surplus) is marketed [30]. In addition, these systems are located in rural areas and have limited data, resources, and different climatic and non-climatic conditions [2]. These thematic groups demonstrate the depth of this systematic review and the extent to which assimilation of RS data has been used in PBCMs worldwide.

3. Results

3.1. Temporal Scope

Over the past decade, there has been an increasing trend in publications focused on improving crop model estimates by integrating RS data from around the world (Figure 2). The number of publications was highest especially in the last three years (2019–2021), accounting for about 45% of the reviewed studies.

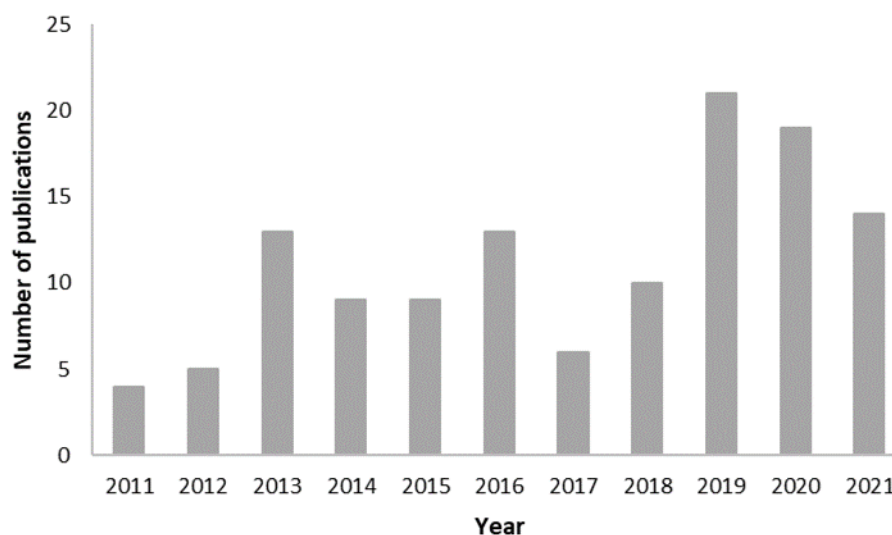


Figure 2. Publication trend between 2011 and 2021.

3.2. Geographical Distribution

Most identified studies that focused on improving crop model estimation by assimilating RS data were conducted in Asia, Europe, and North America (Figure 3), with Asia having the highest proportion (71%). More specifically, these studies were mainly conducted in China (63%) [31,32] and the United States (US) (7%) [33,34]. France [35,36], Germany [37,38], and Italy [39,40] each contributed 5%. In contrast, South America (3%) and Africa (<1%) showed a lack of data assimilation research, with studies conducted only in Brazil [41,42], Uruguay [7,43], and Ethiopia [44]. The geographic distribution of the identified data as-

simulation research seems to reflect regional differences in the progress of and access to agricultural technologies and innovation status. In addition, China, the US, France, and Germany are among the top ten agricultural-producing countries in the world. Thus, the predominance of data assimilation research in Asia, Europe, and North America indicates a focus on relatively advanced regions in agricultural production, technology, and innovation. This also shows where the research groups currently working on data assimilation are located.

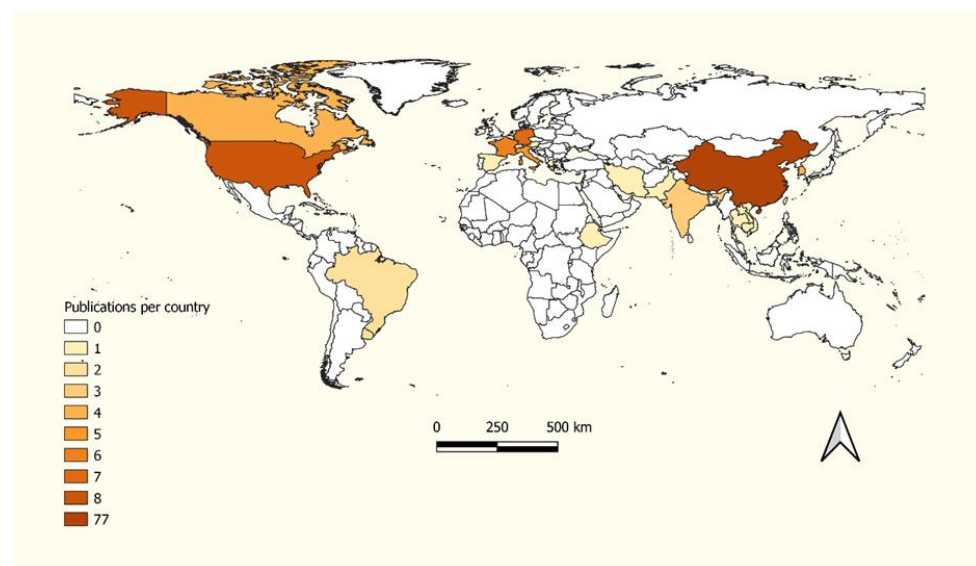


Figure 3. Geographical distribution of the number of reviewed studies per country across the globe.

3.3. Crop Models

The studies reviewed have integrated RS data into many PBCMs to improve crop growth and yield (Tables A1–A3). These include World Food Studies (WOFOST) [45,46], Decision Support System for Agro-technology Transfer (DSSAT) [47,48], a Simple Algorithm For Yield (SAFY) [49,50], AquaCrop [51,52], and Soil Water Atmosphere Plant–World Food Studies (SWAP-WOFOST) [53,54]. Most of these studies used data assimilation to improve crop growth and yield estimates of staple crops (94%), consisting of maize, rice, soybeans, and wheat [55,56] (Tables A1–A3). In addition, other studies examined barley [57], jujube [58,59], and sugarcane [19,60].

3.4. Remote Sensing Datasets

We observed a positive trend in the availability and spatiotemporal details of the RS datasets (Table 2). This trend argues for using RS data for short- and long-term analyses. Most data assimilation studies ($n = 34$) used the Moderate Resolution Imaging Spectroradiometer (MODIS) Terra or Aqua datasets to estimate crop state variables [61,62]. MODIS data have been freely available for decades (since 1999) with a daily temporal resolution. However, they are limited by their low spatial resolution (250–1000 m). Other studies used Landsat datasets ($n = 27$), which have higher spatial resolution (30–120 m) but lower temporal resolution (16 days) [63,64]. With such low temporal resolution, the acquisition of analyzable Landsat imagery may be less frequent and strongly influenced by cloud cover.

Other studies used optical RS datasets with high spatial and temporal resolution, including Sentinel-2 [65,66], Huanjing-1 [67,68], RapidEye [69,70], SPOT-6 [71], and GeoFan-1 [72]. However, the optical satellite sensors only work during the daytime and are limited by weather conditions and vegetation density. In comparison, other studies have used radar RS datasets, such as Sentinel-1 [56] and RadarSAT-2 [73], which are not limited by light availability and can penetrate through clouds and particular vegetation. Recent advances in science and technology have led to the development of unmanned

aerial vehicles (UAVs) and affordable, portable field sensors. Therefore, several studies assimilated have evaluated data from UAVs [54,74] and ASD FieldSpec Spectrometer field sensors [75,76].

Table 2. Remote sensing datasets and their resolutions in the selected papers.

Satellite (Years Active)	Sensor	Spatial Resolution	Temporal Resolution	Total Papers
MODIS (Terra: 1999–present, Aqua: 2002–present)	Terra; Aqua	250–1000 m	1–2 days	34
Landsat-5 (1984–2013)	MSS; TM			
Landsat-7 (1999–present)	ETM	30–120 m	16 days	27
Landsat-8 (2013–present)	OLI; TIRS			
HJ-1 A/B CCD (2009–present)	Optical	30 m	2–4 days	22
Sentinel-1 (2013–present)	Radar	5–60 m	1–5 days	17
Sentinel-2 (2015–present)	Optical			
Field sensors	Multiple	Varies	Varies	13
SPOT 4 (1993–2013)				
SPOT 5 (2002–2015)	Optical	2.5–30 m	1–26 days	11
SPOT 6 (2012–present)				
GLASS (1981–2018)	Multiple	1–5 km	8 days	5
Unmanned aerial vehicle (UAV)	Multiple	Varies	Varies	5
RapidEye (2003–present)	Optical	6.5 m	1–5.5 days	4
GaoFen-1 (2006–present)	Optical	16 m	4 days	3
COMS GOCI (2010–present)	Optical	500 m	Daily	3
RadarSAT-2 (2007–present)	Radar	5–100 m	1–6 days	3
SMOS (2009–present)	MIRAS	35 km	3 days	2
AMSR-E (2002–2011)	Optical	5.4–56 km	Daily	2
FormoSat-2 (2004–2016)	Optical	2–8 m	Daily	2
GEOSAT-1 (2009–present)	Optical	22 m	Daily	1

Note: Some articles used multiple remote sensing datasets, so the total number of datasets is higher than the number of reviewed publications. MSS, TM, ETM, OLI, and TIRS represent Multispectral Scanner, Thematic Mapper, Enhanced Thematic Mapper, Operational Land Imager, Thermal Infrared Sensor, and Microwave Imaging Radiometer with Aperture Synthesis (MIRAS), respectively.

3.5. Data Assimilation Methods and Application Scale

Several single-state variables were selected as assimilation variables, with LAI being the most frequently (54%) assimilated variable in the studies examined (Tables A1–A3). In addition, soil moisture (SM) [41,77], FAPAR [19,72], vegetation indices [78,79], reflectance [69,80], aboveground biomass (AGB) [70], canopy nitrogen accumulation (CNA) [81], phenology [54], and fraction of vegetation cover (fvc) [39] were also assimilated into PBCMs. Other studies combined two or more state variables to improve yield estimates [52,75]. About 21% of studies combined LAI with other state variables such as SM [82,83], sowing date (SD) [45,66], evapotranspiration (ET) [16,63], canopy cover [51,84], CNA [85], AGB [73], leaf nitrogen accumulation (LNA) [86], FAPAR [46], phenology [87], and vegetation indices [32,88] to improve model simulations. Only 4% of studies used the forcing method to incorporate data from RS into PBCMs [60,89] (Tables A1–A3). Meanwhile, 39% of the studies used the recalibration method, mainly using the shuffled complex evolution (SCE) ($n = 20$) [90,91] and particle swarm optimization (PSO) algorithms ($n = 17$) [92,93] to optimize the initial model parameters. Most studies applied the updating method (41%) along with the Ensemble Kalman Filter (EnKF) ($n = 34$) algorithm [94,95] to update the critical model-simulated state

variables. In addition, 3% and 12% of the studies compared recalibration with the forcing and updating methods, respectively [96,97]. About 44% of the studies reviewed applied data assimilation at the regional level, including the district and national levels [98,99], while 33% were conducted at the field level [100,101] (Tables A1–A3). A few studies (3%) were conducted at a sub-field scale, including plot and pixel levels [49,50]. In studies where data assimilation was applied at both the field and regional scales, two experiments were usually performed (20%) [66,102]. The first experiment was conducted at the field scale to illustrate the feasibility of the data assimilation method. The second experiment was conducted at the regional scale to estimate regional yields and analyze the spatial effect of the data assimilation approach.

3.6. Types of Agricultural Cropping Systems

Of all the data assimilation research reviewed, 33% of the studies indicated that they were conducted at national experimental sites, where research was conducted on various sustainable farming practices, such as irrigation requirements [33,59]. About 44% of the studies focused on irrigated agricultural cropping systems [103,104], while 15% were based solely on rainfed agricultural cropping systems [105,106] (Figure 4). In addition, 3% of the studies compared the effect of data assimilation on improving model simulations under rainfed and irrigated systems [64,107]. The remaining studies did not clearly distinguish whether the study was conducted under rainfed or irrigated conditions. Similarly, it was unclear what type of fields were used, as 94% of studies did not indicate whether the data assimilation approach was applied under commercial or small-scale farming systems. Nevertheless, approximately 5% of the studies indicated that they were based on commercial farms [38,43], while less than 1% were based on small-scale systems [44]. Thus, this review shows that most data assimilation studies were based on cropping models under potential conditions.

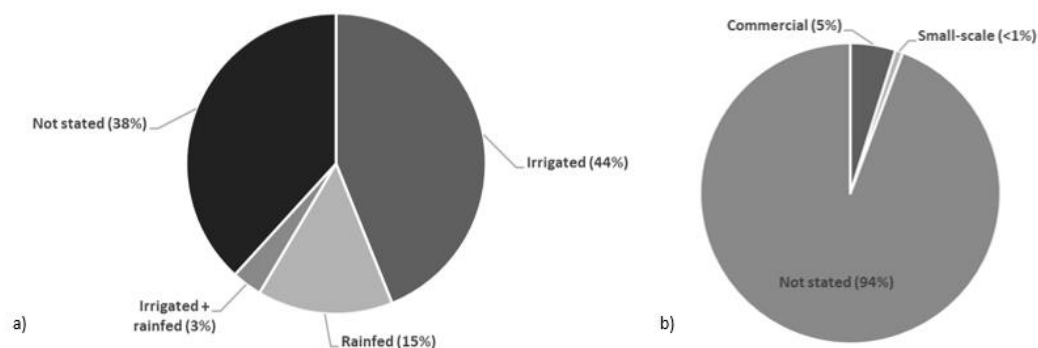


Figure 4. Rainfed versus irrigated (a) and small-scale versus commercial (b) cropping systems.

4. Discussion

4.1. Current Status of Data Assimilation in Remote Sensing and Crop Models

Over the past decade, interest in improving crop model estimates by assimilating RS data has increased worldwide. The highest number of annual studies was conducted between 2018 and 2021 (Figure 2). The more significant number of studies in recent years reflects the growing awareness and demonstrates the benefits of assimilating RS data into PBCMs worldwide. In addition, the last decade has been marked by significant advances in computational capacity and efficiency and individual development of PBCMs and RS technologies. Thus, we expect the interest in integrating RS data into crop models to grow as knowledge of the process improves, and there is a need to estimate crop growth status and yield at regional and national scales.

Our research shows that data assimilation applications are mainly used in Asia, Europe, and North America, with China having the largest share. This is consistent with areas associated with high agricultural technology and innovation. These areas have access to and can use advanced computer software, code, and facilities, as well as the data needed

to calibrate and validate crop models. They can also access the latest satellite data and advanced technologies such as UAVs and portable field sensors. This geographic distribution highlights a notable lack of data assimilation applications in African and South American countries where agricultural crop production significantly contributes to food security, economic growth, and poverty reduction. This gap also highlights the lack of human resources and data capacity to conduct and evaluate such research; thus, there is less capacity to use PBCMs in these areas. Finally, it is vital to investigate the impact of potentially sustainable agricultural land management practices on local crop growth and yields.

4.2. Complementary Advancement of Crop Models and Remote Sensing Datasets

Crop models have evolved from simulating individual plant ecophysiological processes to integrating crop development processes at the field and regional scales. PBCMs, including WOFOST, DSSAT, and AquaCrop, are continuously refined and updated to better assess crop growth status and yield [24]. In addition, many PBCMs are becoming easily accessible using standardized and open-source modeling environments such as Python Crop Simulation Environment (PCSE) (<https://pcse.readthedocs.io/en/stable/>, accessed on 1 July 2022), which facilitates the assimilation of RS datasets [7]. Most studies assimilated data from RS into the WOFOST model. WOFOST has an open-source repository (<https://github.com/ajwdewit/WOFOST>, accessed on 1 July 2022) that provides clear guidelines and methods for incorporating RS data and for the PCSE platform. Despite the renowned development of crop models, they are still more efficient in simulating major crops. However, due to a lack of detailed field data, they have difficulty representing uncommon and underutilized crops such as Bambara groundnut, hemp, and millet [108,109]. Therefore, most studies reviewed used data assimilation to improve growth and yield estimates for mainly staple crops such as maize, rice, soybean, and wheat (Tables A1–A3).

Over the past decade, data sets from RS have evolved significantly due to the expansion of spectral bands, radar sensors, and optical sensors and are now available (Table 2). However, the application of data assimilation is generally limited due to the availability and quality of the data from RS [110]. For example, although relatively high-resolution data from RS can provide accurate estimates of crop variables, they may be limited by scale, repeat time, and the availability of cloud-free imagery [10]. Therefore, most studies in our review still used relatively coarse resolution MODIS data for assimilation because they are freely available and have a short repeat time. Our review was also dominated by studies that assimilated data from Landsat with relatively low temporal resolution but higher spatial resolution. The mismatch between the RS data and the agricultural landscape may reduce data reliability with particularly low spatial and/or temporal resolution.

Nevertheless, satellite data with high spectral, temporal, and spatial resolution from the PlanetScope, Landsat-8, Sentinel-2, and Sentinel-3 series have recently become freely available for research and operational purposes [111,112]. Sentinel-2, for example, has a spatial resolution of 10 m and a repetition time of 1–5 days (Table 2). In addition, multispectral UAVs and affordable field sensors have been introduced that provide non-abstracted data at high spatial and temporal resolution [113]. To date, however, relatively few studies have utilized these high-resolution datasets. In general, the assimilation of high-resolution RS datasets into crop models leads to a more detailed spatial characterization of accurate growth and yield estimates [25]. However, the choice of a high-resolution RS dataset depends on the scale, access, and accuracy required by the user [114]. UAVs, for example, provide relatively low-cost imaging at high spatial resolution, low altitude, and user-preferred temporal resolution [14]. Therefore, they are well suited for field-scale application. However, compared to satellite imagery, UAVs and field sensors have low coverage per image. In contrast, high-resolution space-based, which are relatively expensive (e.g., RapidEye) and susceptible to the influence of cloud cover (e.g., Sentinel-2), provide imagery at higher altitudes and lower temporal resolution [74].

In some studies, high-resolution datasets from multiple sources of RS have been integrated (e.g., the spatial resolution enhancement method) to obtain more accurate spatial

and temporal estimates of crop state variables. For example, combining the Huanjing-1 and RADARSAT-2 datasets with AquaCrop improved the accuracy of wheat biomass (root mean square error (RMSE) = 1.53 t/ha) and yield estimates (RMSE = 0.81 t/ha) than assimilating Huanjing-1 only (biomass RMSE = 2.35 t/ha, yield RMSE = 0.92 t/ha) and RADARSAT-2 only (biomass RMSE = 2.11 t/ha, yield RMSE = 0.86 t/ha) [115]. Similarly, assimilation of LAI from a fusion of Landsat-8 and MODIS data into SAFY resulted in improved estimates of maize (RMSE = 146.34 g/m², coefficient of determination (R²) = 0.56) and soybean (RMSE = 82.86 g/m², R² = 0.54) yields [49].

4.3. Type of Data Assimilation Methods

Among the single-state variables used in data assimilation, LAI is one of the most frequently used variables because it is easily retrieved from RS and captures crop growth limiting and reducing factors. LAI also plays an essential role in accurately representing different developmental stages, accounting for the combined effect of growth environment and management, and determining the biomass and yield estimated within the crop model [31,47,116,117]. However, numerous variables interact within PBCMs and influence the final estimated yield [82]. RS data access and processing for several relevant crop variables have improved significantly over the past decade, allowing multivariate data to be incorporated into PBCMs. A study by [16] found that the joint integration of MODIS LAI and ET variables into the SWAP resulted in more accurate wheat yield estimates than the individual integration of LAI or ET data at the national level. Compared to open-loop estimates (R² = 0.41), [82] found that joint assimilation of LAI and SM from Sentinel-1 and -2 into WOFOST resulted in the most accurate wheat yield estimates by reducing the RMSE by 167 kg/ha (R² = 0.76). Assimilation of only LAI and only SM reduced the yield RMSE by 69 kg/ha (R² = 0.65) and 39 kg/ha (R² = 0.50), respectively. In addition, joint assimilation of LAI and LNC from Landsat-8 into the DSSAT model improved the accuracy of wheat grain protein content prediction (RMSE = 0.91%, R² = 0.39) [118].

In addition, 30% of studies coupled crop models with radiative transfer models (RTMs) during the data assimilation process [113,119]. RTMs, including PROSAIL, A two-layer Canopy Reflectance Model (ACRM), the Markov Chain Reflectance Model (MCRM), the Soil–Leaf–Canopy model (SLC), and the Atmospheric Land Exchange Inverse model (ALEXI), can simulate state parameters such as the LAI needed during the assimilation process [120,121]. This modeling framework directly compares the spectral reflectance obtained from RS datasets with that simulated by RTMs to optimize specific processes or update the initial parameters of the crop model. This leads to more detailed modeling of temporal changes in the spectral reflectance response of the crop canopy and primary crop, water, and nutrient processes [65,102]. Coupling PBCMs with RTMs, therefore, improves estimates of crop growth and yield estimations.

The studies reviewed demonstrate, with varying degrees of success, the advantages and limitations of all three data assimilation approaches. In general, it is relatively easy to integrate data from RS into a crop model using the forcing method (Table 3). The forcing approach is less complex and does not use data assimilation algorithms because the crop model uses a remotely sensed state variable instead of its information and therefore requires less computation time. However, the data from RS may contain measurement errors that can be introduced into the crop model when the forcing method is used. This may reduce the accuracy of the estimated model results. In addition, this method requires many RS observations for each simulation step (i.e., daily or weekly observations), which are rarely available, especially when using data from optical sensors that may be affected by cloud cover [122]. The time of sowing or emergence, which mark the beginning of crop growth, must be accurately determined in advance. In our review, forcing was used in only a few studies. For example, the assimilation of LAI from Sentinel-1 into the ORYZA model using the forcing method resulted in fairly accurate regional rice yield estimates with a normalized root mean square error (NRMSE) of 9.21% and an overall agreement between actual and estimated yield of 83–89% [56].

Table 3. The main difference between the three methods for assimilating remote sensing data into crop models.

	Data Assimilation Method		
	Forcing	Recalibration	Updating
Number of iterations	Fewer	More	Fewer
Computational time	Less	More	Less
Flexibility	No	Yes	Yes
Propagation of uncertainty	Possibly	Minimize errors	Minimize errors
Number of parameters	Fewer	More	More
Complexity	Less	Less	More

In most studies reviewed, the recalibration or updating method was successfully applied. For example, the re-estimation of developmental parameters in SWAP-WOFOST based on phenological information derived from MODIS LAI using the SCE optimization scheme resulted in an improved wheat yield estimate by reducing the RMSE to 5.4% in 2007 and 15.4% in 2008 compared to the method without data assimilation [98]. Assimilation of MODIS LAI into WOFOST based on the two SCE optimization schemes for reinitialization of emergence date, initial AGB, and initial available soil water significantly improved the accuracy of regional wheat yield estimates by reducing the RMSE from 983 kg/ha to 474 kg/ha and 667 kg/ha, respectively, for the two different optimization schemes [123]. In a study by [32], the EnKF algorithm was used to integrate Huanjing-1 LAI into WOFOST to update the simulated LAI, resulting in improved regional rice yield estimates (RMSE = 1.61 t/ha, $R^2 = 0.66$). The recalibration method is mainly used when the RS observations are sufficient and have limited error [58]. It better represents the input model parameters and minimizes the increase in RS error during the assimilation process (Table 3). Therefore, the recalibration method performs better than the updating method in the presence of uncertainties in plant information. However, the disadvantage of the recalibration method is that the optimization iteration process takes too much computation time [124]. The updating method requires relatively less computation time than the recalibration method (Table 3). However, the updating method requires complex calculations. This approach estimates the uncertainty between the model estimate and the RS observation [122]. The accuracy of the estimate and efficiency of the updating method also depends on the date of the selected images and the consistency in the phenological information. For example, [44] concluded that wheat yield estimation is more sensitive to LAI assimilation at the flowering stage. Nevertheless, [53] showed that the EnKF updating method gave a more reliable estimate of sugarcane yield (RMSE = 7.1 t/ha, $R^2 = 0.63$) than the forcing (RMSE = 9.54 t/ha, $R^2 = 0.43$) and calibration (RMSE = 13.89 t/ha, $R^2 = 0.19$) methods.

4.4. Application of Data Assimilation in Small-Scale Agricultural Systems

Data assimilation was applied to several agricultural systems (Figure 4). In our review, studies conducted under irrigated systems dominated as opposed to rainfed systems. Therefore, these studies evaluated crop growth under potential conditions. This is due to the high proportion of studies conducted in China, where irrigated agriculture accounts for a large portion of the country. Over 60% of China's national water resources are used for agricultural irrigation [125]. The country also has several national experimental sites where the effects of various sustainable farming practices, such as irrigation demand and efficiency on crop growth and yield, have been studied [31]. Integrating LAI and SM in the crop model resulted in more accurate yield estimates than integrating each variable individually for rainfed areas. For example, maize yield estimates improved more when both LAI and SM were assimilated into DSSAT (RMSE = 1.8 Mg/ha, $R^2 = 0.65$) compared with open loop ($R^2 = 0.47$) or independent assimilation of LAI (RMSE = 1.1 Mg/ha, $R = 0.51$) or SM ($R = 0.50$, RMSE = 0.5 Mg/ha), especially when estimating yield in years with average rainfall [15]. However, assimilation of only LAI was better at estimating yield in extremely wet years. Similarly, [48] found that assimilation of only LAI did not capture the increased water stress

in rainfed wheat and reduced the accuracy of simulated yield, while assimilation of LAI and SM resulted in the most accurate yield estimate (RMSE = 424.75 kg ha⁻¹, absolute relative error (ARE) = 9.55%).

More than 90% of the studies did not indicate whether they applied data assimilation to commercial or small-scale agricultural systems (Figure 4). Only [44] assimilated MODIS LAI using EnKF in WOFOST to improve wheat yield estimates from small-scale rainfed farming systems in Ethiopia. The lack of such studies can be attributed to crop models inadequately representing uncommon crops and alternative cropping methods (e.g., mixed cropping) usually used by small-scale farmers [6]. In addition, obtaining reliable and sufficient input data for calibration and validation of small-scale farming systems is difficult. Most long-term sensors from RS cannot simultaneously produce images with high spatial and temporal resolution [126]. Therefore, most freely available RS datasets have a low spatial resolution, which limits their application in small-scale agriculture. Scattered, diverse, and disparate plots with a mix of cropping patterns, varying access to technologies and information (e.g., access to climate or agricultural extension), and different management objectives (e.g., commercial or subsistence) typically characterize small-scale systems. Therefore, matching available RS datasets with low spatial resolution to small-scale farming systems' great diversity and spatial detail can be challenging [127].

Nonetheless, satellite-based Earth observation (EO) is moving toward big data cloud platforms. For example, high-resolution datasets such as PlanetScope, Landsat-8, Sentinel-2, and Sentinel-3 show increasing improvements in the findability, accessibility, interoperability, and reusability of RS datasets. On the one hand, access to such standardized processing platforms reduces the effort to access ready-to-use RS-based crop parameters. Still, it requires hardware and software capabilities for processing. Therefore, such high-resolution RS data can be integrated into crop models when studying heterogeneous small-scale cropping systems. Small-scale agricultural systems can also benefit from ultrahigh-resolution multispectral UAVs. Unlike space satellites, UAV imagery is not limited by the effects of cloud cover, as the user sets the temporal resolution that can be adjusted to local weather conditions [54]. UAV imagery can provide observational data on individual crops or patches at very low altitudes, ultimately providing better coverage of the overall patterns and crop variability in fields, as required for small-scale agricultural conditions. Nevertheless, owning and maintaining UAVs could prove expensive and difficult for small-scale farmers, especially in African countries, as they have limited resources and capacity to operate, process, and interpret the collected data. However, a cost-effective alternative to support small-scale farmers could be to opt for community ownership of UAVs and involve extension services [114].

4.5. Future Opportunities

In the last decade, several single-crop models have been used to estimate the growth and yield of various crops under different environmental conditions. However, individual crop models differ in their strengths, structure, complexity, and parameters because they were developed in multiple environments and for different purposes [23,24]. There is a need to compare the performance of different crop models. For example, some studies in this review compared the integration of RS into AquaCrop and SAFY to improve wheat yield estimation [51,84]. There is also a need to combine the advantages of different models to improve the overall applicability and capability of crop models. For example, the Agricultural Model Intercomparison and Improvement Project (AgMIP) consists of several crop modeling groups that evaluate simulation results for specific crops and environmental conditions [128]. Future research can therefore explore the integration of RS data into AgMIP models to improve crop estimation. In addition, the holistic approach of crop models needs to be improved, including consideration of pests and diseases, other cropping practices such as intercropping, and other extreme events such as frost damage and flooding. We also anticipate increasing the application of crop models in climate change research, as crop models can be used to assess the impact of future climate conditions and extreme

events on current agricultural systems. Successful data assimilation results depend on the careful calibration of the model [111]. However, obtaining reliable and sufficient data, as required for complex PBCMs, remains challenging in some areas. Therefore, future research should investigate deriving a simplified model with minimal requirements from complex models. Integrating remote sensing data into crop models is a promising approach to improve crop growth and yield estimation for sustainable crop management strategies. The rapid development of RS technology has increased the availability of satellite datasets with high temporal and spatial resolutions (Table 2). Such datasets can be used with UAVs and portable field sensors to improve dynamic time series simulations of models, reduce the likelihood of mixed pixels, and provide more spectral information to increase the accuracy of crop growth and yield estimates at the field and regional levels. In addition, integrating multiple multispectral datasets with high temporal and spatial resolution or multiple state variables will further improve the accuracy of growth and yield estimates. Further development of data assimilation strategies and algorithms will reduce uncertainties and errors in assimilating RS into crop models. This will improve the accuracy of crop growth and yield estimates.

Prospects of Data Assimilation Research in Africa

Small-scale rainfed agriculture systems dominate the African region and account for about 80% of the food supply in sub-Saharan Africa [129]. Africa and other developing areas, which have large and wide yield gaps compared with the global average, would benefit noticeably from improved capacity to apply PBCM approaches. The results of this study show a lack of research on data assimilation in Africa (Figure 2), as only one study was conducted under these conditions [44]. The overall limited interest in using and exploiting crop models in the region can explain the lack of African studies. This is primarily due to the lack of reliable crop growth data for calibration, validation, and, ultimately, relevance of the model [130,131]. Sometimes the required data are freely available or easy to use. In cases where data are available, they are often of too low quality and quantity to adequately control or validate most crop models [5]. In addition, the use of RS data in African agriculture is limited due to the cost of acquiring imagery [132]. Crop models can provide the opportunity to evaluate agronomic practices [133], yield changes [134], and water productivity [135] under different climates and management practices to improve small-scale rainfed agricultural systems. Despite the known limitations of data from RS, freely available high-resolution RS data, including Sentinel-2, Sentinel-3, PlanetScope, Landsat-8, can be assimilated into crop models to improve crop yield and growth estimates, particularly for small-scale agricultural systems. This access could help address data scarcity conditions, strengthen African scientific community interests by democratizing the use of PBCMs, and gradually lead to efficient modeling and relevant information for the improvement of small-scale heterogeneous agricultural systems. High-resolution RS datasets can be further integrated with UAVs and field sensors [112] to reduce operational costs and produce improved high-resolution multisource data suitable for modeling small-scale agricultural systems. Data assimilation research can therefore enable African small-scale farming systems to further address the need for site-specific and appropriate cropping strategies for sustainable and climate-resilient agricultural development. Therefore, more context-specific application of data assimilation to improve local crop growth and yield estimates for small-scale cropping systems should be conducted throughout Africa.

5. Conclusions

Globally, there is growing interest in approaches and applications to better assess crop growth and yield. We are seeing increasing development of crop models, availability of RS data sources (with increasing detail), and characterization of potential state variables. However, the application of data assimilation has followed the trend of agricultural production, technology, and innovation, with more studies conducted in technologically advanced countries than in less developed counties (e.g., those in Africa). Most studies use

recalibration or updating methods along with various algorithms to incorporate mainly remotely sensed LAI data into crop models. Generally, the excessive computation time required during the iteration process limits these methods. However, a cloud-based implementation will reduce this by providing ready-to-use EO crop parameters or distributing data processing. Data assimilation has mainly been used to improve yield estimates for staple crops in irrigated farming systems, while evaluations were not sufficiently performed for rainfed systems and other important crops such as Bambara groundnut and millet. The application of data assimilation in small-scale agricultural systems remains a challenge due to the limited use of and access to crop models and remote sensing data at high spatial resolutions that match the diversity, dispersion, and non-uniformity of small-scale agricultural systems. However, the newly available high-resolution datasets such as UAVs, PlanetScope, Landsat-8, Sentinel-2, and Sentinel-3 provide opportunities to address the resolution problem. In addition, integrating multiple multispectral datasets with high temporal and spatial resolution or multiple state variables into crop models will further improve the accuracy of growth and yield estimates for small-scale agricultural systems. Therefore, further research should investigate how published approaches to large-scale and new high-resolution RS data can be used for small-scale agricultural systems. Additional research is also needed to evaluate the parameters to assimilate, the assimilation strategies, and the different crop models needed to estimate crop yields and the growth of small-scale farming systems appropriately. This is key to making informed decisions about the local crop management required to improve food policy and assess food security, especially in small-scale farming systems and developing countries.

Author Contributions: Conceptualization, L.D., O.C. and J.v.D.; methodology, formal analysis, data curation, writing—original draft preparation, visualization, L.D.; writing—review and editing, O.C., J.v.D. and L.K.; supervision, O.C. and J.v.D. All authors have read and agreed to the published version of the manuscript.

Funding: This research was funded by an NRF-NUFFIC Doctoral Scholarship (Split Site Mode), NRF-GCSSRP, an ARUA-CD Scholarship, and an ATAP Scholarship.

Data Availability Statement: The data presented in this study are openly available in 4TU.ResearchData at https://data.4tu.nl/private_datasets/4dvmzBUFkO9H5-XxnyrC8P1c6Z_GgI0B-5_qqGU2SZo.

Conflicts of Interest: The authors declare no conflict of interest.

Appendix A

Table A1. Analysis of publications that applied the forcing method.

Crop	CGM	RS Data	State Variable	Scale	Aim	Reference
Jujube	WOFOST	Landsat-8	LAI	Field	Yield, AGB	[59]
Rice	STICS	SPOT-4, SPOT-5, Landsat-8	LAI	Field	AGB, SD	[35]
Rice	STICS + <i>PROSAIL</i>	Sentinel-2	LAI, SD	Field, regional	Yield	[66]
Wheat	DSSAT	Landsat-7, Landsat-8	NDWI	Field, regional	Yield, SM	[64]
Wheat	SAFY	Sentinel-2, PlanetScope	LAI	Field	Yield	[89]
Rice	ORYZA	Sentinel-1	LAI	Regional	Yield	[56]
Sugarcane	MOSICAS	SPOT-4, SPOT-5	NDVI	Field	Yield	[60]
Sugarcane	MOSICAS	SPOT-4, SPOT-5	FAPAR	Field	Yield	[19]
Sugarcane	SWAP-WOFOST	UAV	LAI, SM	Field	Yield	[53]
Wheat	WOFOST	SPOT-VGT	LAI, SD	Regional	Yield	[45]

Note: LAI, SD, AGB, NDWI, NDVI, and FAPAR represent leaf area index, sowing date, above-ground biomass, normalized difference water index, normalized difference vegetation index, and the fraction of absorbed photo-synthetically active radiation, respectively.

Table A2. Analysis of publications that applied the recalibration method.

Crop	Model	RS Data	State Variable	Assimilation Algorithm	Scale	Aim	Reference
Jujube	WOFOST	Landsat-8	LAI	SUBPLEX	Field	Yield	[58]
Jujube	WOFOST	Landsat-8	LAI	SCE	Field	Yield, AGB	[59]
Soybean	SAFY	Radarsat-2, Formosat-2, SPOT-4, SPOT-5	LAI, AGB	Simplex	Field	Yield, AGB	[73]
Wheat	AquaCrop + PROSAIL	Huanjing-1, Landsat-8	LAI, CC	Simplex	Field	Yield	[119]
Wheat	AquaCrop + PROSAIL	Huanjing-1, Landsat-8	LAI, CC	Simplex	Field	Yield	[51]
Wheat	DSSAT	Landsat-8	LAI, LNA	SCE, SA, DE	Regional	GPC	[118]
Rice	STICS + PROSAIL	Sentinel-2	LAI, SD	Simplex	Field, regional	Yield	[66]
Wheat	DSSAT + PROSAIL	Field sensor	Reflectance, NDVI	VFSA	Field	LAI	[75]
Wheat	DSSAT + PROSAIL	Field sensor	Reflectance, NDVI	VFSA	Field	LAI	[104]
Rice	WARM + PROSAIL	Landsat-7, Landsat-8	LAI	Simplex	Field	Yield	[136]
Wheat	WOFOST + PROSAIL	Landsat-8, MODIS	Reflectance	SCE	Field, regional	Yield	[80]
Wheat	SAFY + ESTARFM	Landsat-8, MODIS	GLAI	SCE	Field	AGB	[91]
Maize	DSSAT + MCRM	MODIS	LAI, EVI	GA	Regional	Yield	[88]
Wheat	WOFOST	MODIS	LAI	SCE	Field, regional	LAI, MD	[137]
Wheat	SAFY	Landsat-7, Landsat-8, Sentinel-2	LAI	ULM	Field	Yield	[43]
Soybean	WOFOST	Sentinel-2	LAI	SUBPLEX	Field	Yield	[7]
Wheat	SWAP- WOFOST	MODIS	LAI, ET	SCE	Field, regional	Yield	[63]
Wheat	SWAP- WOFOST	MODIS	LAI, ET	SCE	Field, regional	Yield	[16]
Wheat, Maize, Soybean	STICS	Landsat-7, SPOT-5	LAI	Simplex	Field	Yield, AGB	[55]
Maize	STICS	Landsat-7, SPOT-5, CASI	LAI	Simplex	Regional	Yield, SWC	[105]
Rice	GRAMI	COMS GOCI, MODIS	LAI	POWELL, Quasi-Newton	Regional	ET, GPP	[138]
Rice	WOFOST	Landsat-8	LAI	PSO	Regional	WRT	[93]
Wheat	AquaCrop	Field sensor	NDMI	PSO	Regional	Yield, AGB	[76]
Wheat	AquaCrop	Huanjing-1, MODIS	LAI, AGB, EVI, RVI, MTV12	PSO	Regional	Yield, AGB, CC	[115]
Maize	AquaCrop	Field sensor	CC, AGB	PSO	Sub-field	Yield	[52]
Maize	DSSAT	RapidEye	AGB	SA	Field	Yield	[70]
Wheat	DSSAT	Field sensor	CNA	PSO	Regional	Yield, GPC	[81]
Wheat	DSSAT	Field sensor	LAI, CNA	PSO	Regional	Yield, GPC	[85]
Wheat	WOFOST	MODIS	LAI	SCE	Regional	Yield	[123]
Rice	SIMRIW	COSMO- SkyMed	LAI	Simplex	Regional	Yield	[116]
Sugarcane	MOSICAS	SPOT-4, SPOT-5	FAPAR	SA	Field	Yield	[19]
Rice	GRAMI	COMS GOCI, RapidEye	LAI	POWELL, Quasi- Newton	Field, regional	Yield	[106]
Rice	GRAMI	COMS GOCI, RapidEye	LAI	POWELL, Quasi- Newton	Regional	Yield	[139]

Table A2. Cont.

Crop	Model	RS Data	State Variable	Assimilation Algorithm	Scale	Aim	Reference
Wheat	EPIC + PROSAIL	Sentinel-2	LAI	Fmincon	Field, regional	Yield	[111]
Wheat	EPIC	MODIS	LAI	SCE	Regional	Yield, SD	[61]
Soybean	GRAMI	Field sensor	LAI	POWELL	Field	Yield	[101]
Wheat	AquaCrop + PROSAIL	Huanjing-1, Landsat-8	LAI, CC	PSO	Field, regional	Yield	[84]
Rice	DSSAT	MODIS	LAI	PSO	Regional	Yield	[92]
Wheat	DSSAT + PROSAIL	Field sensor	LAI	PEST, GA	Field	Yield, CC, CNA	[120]
Wheat	WFOST	MODIS.	LAI	POWELL, SCE	Field, regional	Yield	[33]
Sunflower	SUNFLOW	GEOSAT-1, Formosat-2, Landsat-8, Sentinel-2, SPOT-5	LAI	LSE	Field	Yield	[36]
Wheat	AquaCrop	Sentinel-2	CC	PSO	Field	Yield	[140]
Maize	MCWLA	GLASS, MODIS	LAI, VTCI	GA	Regional	Yield	[32]
Rice	RiceGrow	Field sensor, Huanjing-1	LNA, LAI	PSO, SCE	Field, regional	Yield	[86]
Wheat	WFOST + PROSAIL	MODIS	GAI	Simplex	Regional	Yield, AGB	[96]
Wheat	WFOST + PROSAIL	GaoFen-1, Huanjing-1	LAI	SCE	Field, regional	Yield	[117]
Wheat	WFOST + PROSAIL	GaoFen-1, Huanjing-1	LAI	SCE	Field, regional	Yield, SM	[97]
Wheat	SWAP-WFOST	MODIS	LAI	SCE	Regional	Phenology	[98]
Wheat	SAFY	Field sensor	LAI	SCE	Field	LAI, AGB	[50]
Wheat	MCWLA	GLASS	LAI, SM, phenology	PSO	Regional	Yield	[68]
Wheat	SAFY	Field sensor	LAI	SCE	Field	Yield, ET, AGB, SM	[90]
Rice	WFOST	Huanjing-1	LAI	PSO	Regional	WSO, WRT	[141]
Wheat	WFOST	Huanjing-1, Landsat-8	LAI	LSM	Regional	Yield	[142]
Wheat	DSSAT	ESACCI, MODIS	SM, LAI	SCE-UA	Field	Yield	[143]
Wheat	WFOST	MODIS	LAI	SCE-UA	Regional	MD, anthesis	[62]
Wheat	WheatGrow + PROSAIL	HUANJING-1	NDVI, RVI, SAVI, EVI, LAI, LAN	PSO	Regional	LAI, LNA, Yield	[79]
Maize	DSSAT	Field sensor	LAI	VFSA	Regional	LAI	[144]
Wheat	AquaCrop	Sentinel-2	CC	PSO	Field	Yield	[37]
Wheat	WheatGrow + PROSAIL	Huanjing-1, SPOT-5, SPOT-6	RVI, NDVI, SAVI, EVI	LUT	Regional	Yield, LAI, LNA	[78]
Rice	MCWLA	GLASS	LAI, phenology	PSO	Regional	Yield, phenology	[87]
Rice	WFOST + PROSAIL	GaoFen-1	FAPAR	PSO	Regional	FAPAR	[72]
Wheat	PROMET + SLC	Landsat-7, RapidEye	LAI	LUT	Field	Yield	[121]
Rice	STICS	SPOT-4, SPOT-5, Landsat-8	LAI	Simplex	Field	AGB, SD	[35]
Soybean, maize	SAFY + STARFM	Landsat-8, MODIS	GLAI	SCE	Subfield	Yield, AGB, phenology	[49]

Table A2. *Cont.*

Crop	Model	RS Data	State Variable	Assimilation Algorithm	Scale	Aim	Reference
Wheat	WOFOST	Landsat-8, MODIS	LAI	SCE	Field, regional	Yield	[145]

Note: AGB, LNA, EVI, NDVI, RVI, SAVI, GLAI, CNA, CC, VTCI, SM, FAPAR, GPC, MD, ET, GPP, WRT, WSO represent above-ground biomass, leaf nitrogen accumulation, enhanced vegetation index, normalized difference vegetation index, radar vegetation index, soil-adjusted vegetation index, green leaf area index, canopy nitrogen accumulation, canopy cover, vegetation temperature condition index, soil moisture and fraction of absorbed photosynthetically active radiation, grain protein content, maturity date, evapotranspiration, gross primary production, root weight, panicle weight, respectively. SCE-UA, DE, GA, ULM, PSO, LUT, VFSA, PEST, and LSM, respectively, represent optimization algorithms shuffled complex evolution from the University of Arizona, differential evolution, genetic algorithm, unconstrained Levenberg–Marquardt algorithm, particle swarm optimization, look-up-table, very fast simulated annealing, parameter estimation, and least square method.

Table A3. Analysis of publications that applied the updating method.

Crop	Model	RS Dataset	State Variable	Assimilation Algorithm	Scale	Aim	Reference
Jujube	WOFOST	Landsat-8	LAI	EnKF	Field	Yield	[58]
Wheat	WOFOST	MODIS	LAI	EnKF	Field, regional	Yield	[44]
Wheat	AquaCrop + PROSAIL	Huanjing-1, Landsat-8	LAI, CC	EnKF	Field	Yield	[119]
Wheat	AquaCrop + PROSAIL	Huanjing-1, Landsat-8	LAI, CC	EnKF	Field	Yield	[51]
Soybean	DSSAT	SMOS	SM	EnKF	Regional	LAI, GW	[41]
Wheat	MCWLA	Copernicus, GLASS, GLOBMAP	LAI	4DVAR, En4DVAR	Regional	Yield	[22]
Wheat	MCWLA	GLASS	LAI	KF	Regional	Yield	[110]
Maize	WOFOST + PROSAIL	Huanjing-1	LAI	EnKF	Field	Yield	[67]
Maize	WOFOST	Huanjing-1	LAI	EnKF	Field, regional	SAN	[146]
Maize	WOFOST	Huanjing-1	LAI	EnKF	Regional	SAN	[95]
Maize	WOFOST	UAV	LAI	EnKF	Regional	LAI	[113]
Maize	DSSAT	SMAP	SM	EnKF	Regional	Yield, IA	[107]
Wheat	WheatGrow + PROSAIL	Huanjing-1, SPOT6	LAI	EnKF	Field, regional	LNA, Yield	[71]
Wheat	DSSAT + PROSAIL	Field sensor	Reflectance, NDVI	EnKF, 4DVAR	Field	LAI	[75]
Wheat	DSSAT + PROSAIL	Field sensor	Reflectance, NDVI	4DVAR	Field	LAI	[104]
Wheat	WheatGrow	Landsat-5	LAI, LNA	EnSRF, EnKF	Regional	Yield	[147]
Wheat	WOFOST + PROSAIL	Landsat-5, Landsat-8	LAI	4DVAR	Regional	Yield	[148]
Wheat	WOFOST	Landsat-5, MODIS	LAI	EnKF, KF	Regional	Yield	[10]
Wheat	WOFOST	Landsat-8, MODIS	LAI	4DVAR	Field, regional	Yield	[145]
Wheat	WOFOST + PROSAIL	Landsat-8, MODIS	Reflectance	4DVAR	Field, regional	Yield	[80]
Maize	DSSAT	AMSR-E	SM	EnKF	Field, regional	Yield	[15]
Wheat	WOFOST + CASA	Sentinel-2	LAI, FAPAR	EnKF	Field	Yield, NPP	[46]
Wheat	DSSAT + ACRM	Huanjing-1	LAI	PF	Field, regional	Yield	[102]
Wheat	DSSAT + ACRM	Huanjing-1	LAI	POD4DVar	Field, regional	Yield	[149]

Table A3. Cont.

Crop	Model	RS Dataset	State Variable	Assimilation Algorithm	Scale	Aim	Reference
Maize	SAFY	Landsat-5, Landsat-7, Landsat-8	LAI	EnKF	Field	Yield, AGB	[34]
Wheat	DSSAT + PROSAIL	Field sensor	LAI	EnKF	Field	NDVI	[47]
Maize	WOFOST	Landsat-7 GaoFen-1,	LAI	EnKF	Regional	Yield	[103]
Wheat	DSSAT + PROSAIL	Huanjing-1, Landsat-8	LAI	PF, POD4Dvar	Field	Yield	[124]
Wheat	DSSAT + ACRM	Huanjing-1	LAI	EnKF	Field, regional	Yield, phenology	[150]
Wheat	WOFOST	MODIS	LAI	PF	Field, regional	Yield	[31]
Soybean	DSSAT + MIMICS	MODIS	SM, LAI, AGB	EnKF	Regional	LAI, AGB	[151]
Maize	DSSAT	AMSR-E, SMOS	SM	EnKF	Field	Yield	[77]
Wheat	DSSAT	Sentinel-2	LAI, SM	EnKF	Field, regional	Yield	[48]
Wheat	DSSAT	Sentinel-2	LAI	EnKF	Field, regional	Yield	[83]
Wheat	WOFOST + ACRM	Huanjing-1	NDVI	EnKF	Regional	Yield	[152]
Maize	APSIM + PROSAIL	RapidEye	CSF	PF	Field	AGB	[69]
Maize	DSSAT + ALEXI	RDSMP	SM	EnKF	Regional	Yield	[94]
Wheat, barley	SWAP- WOFOST	MODIS	LAI	KF	Regional	Yield, AGB	[57]
Wheat	WOFOST + PROSAIL	Sentinel-1, Sentinel-2	LAI, SM	EnKF	Field, regional	Yield	[82]
Maize	SAFY	UAV	LAI	EnKF	Field	Yield	[14]
Sugarcane	SWAP- WOFOST	UAV	LAI, SM	EnKF	Field	Yield	[53]
Maize	SAFY	Sentinel-2	LAI	EnKF	Field	Yield, AGB	[40]
Wheat	SIMPLACE- LINTUL5 + PROSAIL	Sentinel-2	LAI	EnKF, WM	Sub-field	AGB	[65]
Wheat	SIMPLACE- LINTUL5 + PROSAIL	Sentinel-2	LAI	EnKF	Sub-field	AGB, water stress	[38]
Sunflower	SUNFLOW	GEOSAT-1, Formosat-2, Landsat-8, Sentinel-2, SPOT-5	LAI	EnKF	Field	Yield	[36]
Wheat	AquaCrop	Sentinel-2	CC	EnKF	Field	Yield	[140]
Wheat	AquaCrop	VEN μ S	fvc	DREAM(KZS)	Regional	Yield, AGB	[39]
Maize	WOFOST	Field sensor	LAI	EnKF	Regional	Yield, GPP	[153]
Wheat	DSSAT	MODIS	VTCl	4DVAR	Field, regional	Yield	[154]
Wheat	WOFOST	MODIS	LAI	EnKF	Field, regional	Yield	[155]
Rice	WOFOST	Huanjing-1	LAI	EnKF	Regional	Yield	[32]
Wheat	AquaCrop	Sentinel-2	CC	KF	Field	Yield	[37]
Wheat	WOFOST + PROSAIL	MODIS	GLAI	EnKF	Regional	Yield, AGB	[96]
Wheat	WOFOST	MODIS	LAI	EnKF	Regional	Yield	[156]
Wheat	SAFY	Field sensor	LAI	EnKF	Field	Yield, SM, AGB, ET	[90]
Wheat	WOFOST + PROSAIL	GaoFen-1, Huanjing-1	LAI	EnKF, EnSRF, VW-4DEnSRF	Regional	Yield, SM	[97]

Table A3. Cont.

Crop	Model	RS Dataset	State Variable	Assimilation Algorithm	Scale	Aim	Reference
Sugarcane	SWAP-WOFOST	UAV	Phenology	IES	Field	Yield	[54]
Wheat	AquaCrop	UAV	CC	PF	Field	CC, cdc	[74]
Wheat	WOFOST	Sentinel-2	SM	EnKF	Regional	Yield	[72]
Maize	WOFOST	MODIS	LAI	EnKF	Regional	Yield, GD	[142]
Maize, wheat	WOFOST	MODIS	LAI	EnKF	Field	LAI	[100]
Wheat	WOFOST	Sentinel-1, Sentinel-2	SM	EnKF	Regional	Yield	[157]

Note: SM, LNA, FAPAR, AGB, NDVI, fvc, VTCI, CC, GW, SAN, IA, NPP, GPP, and GD, respectively, represent soil moisture, leaf nitrogen accumulation, fraction of absorbed photosynthetically active radiation, above-ground biomass, normalized difference vegetation index, fraction of vegetation cover, vegetation temperature condition index, canopy cover, grain weight, soil available nutrients, irrigation amount, net primary productivity, gross primary production and growth duration. EnKF, 4DVAR, KF, EnSRF, PF, POD4DVar, WM, DREAM, 4DEnSRF, and IES, respectively, represents updating algorithm ensemble Kalman filter, four-dimensional variational data assimilation, ensemble square root filter, particle filter, proper orthogonal decomposition technique into 4DVar, weighted mean, differential evolution adaptive Metropolis, four-dimensional variational into EnSRF, and iterative ensemble smoother.

References

- Morton, J.F. The impact of climate change on smallholder and subsistence agriculture. *Proc. Natl. Acad. Sci. USA* **2007**, *104*, 19680–19685. [[CrossRef](#)] [[PubMed](#)]
- Williams, P.A.; Crespo, O.; Abu, M.; Simpson, N.P. A systematic review of how vulnerability of smallholder agricultural systems to changing climate is assessed in Africa. *Environ. Res. Lett.* **2018**, *13*, 103004. [[CrossRef](#)]
- Choruma, D.; Balkovic, J.; Odume, O.N. Calibration and Validation of the EPIC Model for Maize Production in the Eastern Cape, South Africa. *Agronomy* **2019**, *9*, 494. [[CrossRef](#)]
- He, M.; Kimball, J.; Maneta, M.; Maxwell, B.; Moreno, A.; Beguería, S.; Wu, X. Regional Crop Gross Primary Productivity and Yield Estimation Using Fused Landsat-MODIS Data. *Remote Sens.* **2018**, *10*, 372. [[CrossRef](#)]
- Kephe, P.N.; Ayisi, K.K.; Petja, B.M. Challenges and opportunities in crop simulation modelling under seasonal and projected climate change scenarios for crop production in South Africa. *Agric. Food Secur.* **2021**, *10*, 10. [[CrossRef](#)]
- Nagamani, K.; Nethaji Mariappan, V.E. Remote Sensing, GIS and Crop Simulation Models—A Review. *Int. J. Curr. Res. Biosci. Plant Biol.* **2017**, *4*, 80–92. [[CrossRef](#)]
- Gasó, D.V.; de Wit, A.; Berger, A.G.; Kooistra, L. Predicting within-field soybean yield variability by coupling Sentinel-2 leaf area index with a crop growth model. *Agric. For. Meteorol.* **2021**, *308–309*, 108553. [[CrossRef](#)]
- Enekel, M.; Reimer, C.; Dorigo, W.; Wagner, W.; Pfeil, I.; Parinussa, R.; De Jeu, R. Combining satellite observations to develop a global soil moisture product for near-real-time applications. *Hydrol. Earth Syst. Sci.* **2016**, *20*, 4191–4208. [[CrossRef](#)]
- Marin, F.; Jones, J.W.; Boote, K.J. A Stochastic Method for Crop Models: Including Uncertainty in a Sugarcane Model. *Agron. J.* **2017**, *109*, 483–495. [[CrossRef](#)]
- Huang, J.X.; Sedano, F.; Huang, Y.B.; Ma, H.Y.; Li, X.L.; Liang, S.L.; Tian, L.Y.; Zhang, X.D.; Fan, J.L.; Wu, W.B. Assimilating a synthetic Kalman filter leaf area index series into the WOFOST model to improve regional winter wheat yield estimation. *Agric. For. Meteorol.* **2016**, *216*, 188–202. [[CrossRef](#)]
- Fang, H.L.; Liang, S.L.; Hoogenboom, G.; Teasdale, J.; Cavigelli, M. Corn-yield estimation through assimilation of remotely sensed data into the CSM-CERES-Maize model. *Int. J. Remote Sens.* **2008**, *29*, 3011–3032. [[CrossRef](#)]
- Yao, F.; Tang, Y.; Wang, P.; Zhang, J. Estimation of maize yield by using a process-based model and remote sensing data in the Northeast China Plain. *Phys. Chem. Earth Parts A/B/C* **2015**, *87–88*, 142–152. [[CrossRef](#)]
- Yuping, M.; Shili, W.; Li, Z.; Yingyu, H.; Liwei, Z.; Yanbo, H.; Futang, W. Monitoring winter wheat growth in North China by combining a crop model and remote sensing data. *Int. J. Appl. Earth Obs. Geoinf.* **2008**, *10*, 426–437. [[CrossRef](#)]
- Peng, X.S.; Han, W.T.; Ao, J.Y.; Wang, Y. Assimilation of LAI Derived from UAV Multispectral Data into the SAFY Model to Estimate Maize Yield. *Remote Sens.* **2021**, *13*, 17. [[CrossRef](#)]
- Ines, A.V.M.; Das, N.N.; Hansen, J.W.; Njoku, E.G. Assimilation of remotely sensed soil moisture and vegetation with a crop simulation model for maize yield prediction. *Remote Sens. Environ.* **2013**, *138*, 149–164. [[CrossRef](#)]
- Huang, J.X.; Ma, H.Y.; Su, W.; Zhang, X.D.; Huang, Y.B.; Fan, J.L.; Wu, W.B. Jointly Assimilating MODIS LAI and ET Products Into the SWAP Model for Winter Wheat Yield Estimation. *IEEE J. Sel. Top. Appl. Earth Obs. Remote Sens.* **2015**, *8*, 4060–4071. [[CrossRef](#)]
- Camino, C.; González-Dugo, V.; Hernández, P.; Sillero, J.C.; Zarco-Tejada, P.J. Improved nitrogen retrievals with airborne-derived fluorescence and plant traits quantified from VNIR-SWIR hyperspectral imagery in the context of precision agriculture. *Int. J. Appl. Earth Obs. Geoinf.* **2018**, *70*, 105–117. [[CrossRef](#)]

18. Clevers, J.; Kooistra, L.; van den Brande, M. Using Sentinel-2 Data for Retrieving LAI and Leaf and Canopy Chlorophyll Content of a Potato Crop. *Remote Sens.* **2017**, *9*, 405. [[CrossRef](#)]
19. Morel, J.; Begue, A.; Todoroff, P.; Martine, J.-F.; Lebourgeois, V.; Petit, M. Coupling a sugarcane crop model with the remotely sensed time series of fIPAR to optimise the yield estimation. *Eur. J. Agron.* **2014**, *61*, 60–68. [[CrossRef](#)]
20. Mishra, V.; Cruise, J.; Mecikalski, J.; Hain, C.; Anderson, M. A Remote-Sensing Driven Tool for Estimating Crop Stress and Yields. *Remote Sens.* **2013**, *5*, 3331–3356. [[CrossRef](#)]
21. Battude, M.; Al Bitar, A.; Morin, D.; Cros, J.; Huc, M.; Marais Sicre, C.; Le Dantec, V.; Demarez, V. Estimating maize biomass and yield over large areas using high spatial and temporal resolution Sentinel-2 like remote sensing data. *Remote Sens. Environ.* **2016**, *184*, 668–681. [[CrossRef](#)]
22. Chen, Y.; Tao, F.L. Improving the practicability of remote sensing data-assimilation-based crop yield estimations over a large area using a spatial assimilation algorithm and ensemble assimilation strategies. *Agric. For. Meteorol.* **2020**, *291*, 14. [[CrossRef](#)]
23. Huang, J.X.; Gomez-Dans, J.L.; Huang, H.; Ma, H.Y.; Wu, Q.L.; Lewis, P.E.; Liang, S.L.; Chen, Z.X.; Xue, J.H.; Wu, Y.T.; et al. Assimilation of remote sensing into crop growth models: Current status and perspectives. *Agric. For. Meteorol.* **2019**, *276*, 16. [[CrossRef](#)]
24. Jin, X.L.; Kumar, L.; Li, Z.H.; Feng, H.K.; Xu, X.G.; Yang, G.J.; Wang, J.H. A review of data assimilation of remote sensing and crop models. *Eur. J. Agron.* **2018**, *92*, 141–152. [[CrossRef](#)]
25. Kasampalis, D.A.; Alexandridis, T.K.; Deva, C.; Challinor, A.; Moshou, D.; Zalidis, G. Contribution of Remote Sensing on Crop Models: A Review. *J. Imaging* **2018**, *4*, 19. [[CrossRef](#)]
26. Sun, P.; Wu, Y.; Xiao, J.; Hui, J.; Hu, J.; Zhao, F.; Qiu, L.; Liu, S. Remote sensing and modeling fusion for investigating the ecosystem water-carbon coupling processes. *Sci. Total Environ.* **2019**, *697*, 134064. [[CrossRef](#)]
27. Livoreil, B.; Glanville, J.; Haddaway, N.R.; Bayliss, H.; Bethel, A.; de Lachapelle, F.F.; Robalino, S.; Savilaakso, S.; Zhou, W.; Petrokofsky, G.; et al. Systematic searching for environmental evidence using multiple tools and sources. *Environ. Evid.* **2017**, *6*, 23. [[CrossRef](#)]
28. Onyango, C.M.; Nyaga, J.M.; Wetterlind, J.; Soderstrom, M.; Piikki, K. Precision Agriculture for Resource Use Efficiency in Smallholder Farming Systems in Sub-Saharan Africa: A Systematic Review. *Sustainability* **2021**, *13*, 1158. [[CrossRef](#)]
29. Spires, M.; Shackleton, S.; Cundill, G. Barriers to implementing planned community-based adaptation in developing countries: A systematic literature review. *Clim. Dev.* **2014**, *6*, 277–287. [[CrossRef](#)]
30. Barnett, A.; Blas, E.; Whiteside, A. AIDS briefs: Subsistence agriculture. In *USAID Health and Human Resources Analysis and Research for Africa Project*; World Health Organization: Washington, DC, USA, 1997.
31. Liu, J.; Huang, J.; Tian, L.; Su, W. Particle filter-based assimilation algorithm for improving regional winter wheat yield estimation. *Sens. Lett.* **2014**, *12*, 763–769. [[CrossRef](#)]
32. Wang, L.; Wang, P.; Liang, S.; Zhu, Y.; Khan, J.; Fang, S. Monitoring maize growth on the North China Plain using a hybrid genetic algorithm-based back-propagation neural network model. *Comput. Electron. Agric.* **2020**, *170*, 12. [[CrossRef](#)]
33. Tian, L.Y.; Li, Z.X.; Huang, J.X.; Wang, L.M.; Su, W.; Zhang, C.; Liu, J.M. Comparison of Two Optimization Algorithms for Estimating Regional Winter Wheat Yield by Integrating MODIS Leaf Area Index and World Food Studies Model. *Sens. Lett.* **2013**, *11*, 1261–1268. [[CrossRef](#)]
34. Kang, Y.H.; Ozdogan, M. Field-level crop yield mapping with Landsat using a hierarchical data assimilation approach. *Remote Sens. Environ.* **2019**, *228*, 144–163. [[CrossRef](#)]
35. Courault, D.; Ruget, F.; Talab-ou-Ali, H.; Hagolle, O.; Delmotte, S.; Barbier, J.-M.; Boschetti, M.; Mouret, J.-C. Combining crop model and remote sensing data at high resolution for the assessment of rice agricultural practices in the South-Eastern France (Take 5 experiment SPOT4-SPOT5). In *Proceedings of the Living Planet Symposium, Prague, Czech Republic, 9–13 May 2016*; p. 171.
36. Trepos, R.; Champolivier, L.; Dejoux, J.F.; Al Bitar, A.; Casadebaig, P.; Debaeke, P. Forecasting Sunflower Grain Yield by Assimilating Leaf Area Index into a Crop Model. *Remote Sens.* **2020**, *12*, 23. [[CrossRef](#)]
37. Wagner, M.P.; Taravat, A.; Oppelt, N. Particle swarm optimization for assimilation of remote sensing data in dynamic crop models. In *Remote Sensing for Agriculture, Ecosystems, and Hydrology XXI*; SPIE: Bellingham, WA, USA, 2019; pp. 174–183.
38. Tewes, A.; Montzka, C.; Nolte, M.; Krauss, G.; Hoffmann, H.; Gaiser, T. Assimilation of Sentinel-2 Estimated LAI into a Crop Model: Influence of Timing and Frequency of Acquisitions on Simulation of Water Stress and Biomass Production of Winter Wheat. *Agronomy* **2020**, *10*, 22. [[CrossRef](#)]
39. Upreti, D.; Pignatti, S.; Pascucci, S.; Tolomio, M.; Huang, W.J.; Casa, R. Bayesian Calibration of the Aquacrop-OS Model for Durum Wheat by Assimilation of Canopy Cover Retrieved from VEN mu S Satellite Data. *Remote Sens.* **2020**, *12*, 23. [[CrossRef](#)]
40. Silvestro, P.C.; Casa, R.; Hanus, J.; Koetz, B.; Rascher, U.; Schuettemeyer, D.; Siegmann, B.; Skokovic, D.; Sobrino, J.; Tudoroiu, M. Synergistic Use of Multispectral Data and Crop Growth Modelling for Spatial and Temporal Evapotranspiration Estimations. *Remote Sens.* **2021**, *13*, 25. [[CrossRef](#)]
41. Chakrabarti, S.; Bongiovanni, T.; Judge, J.; Zotarelli, L.; Bayer, C. Assimilation of SMOS Soil Moisture for Quantifying Drought Impacts on Crop Yield in Agricultural Regions. *IEEE J. Sel. Top. Appl. Earth Obs. Remote Sens.* **2014**, *7*, 3867–3879. [[CrossRef](#)]
42. Liu, F.; Liu, X.N.; Wu, L.; Xu, Z.; Gong, L. Optimizing the Temporal Scale in the Assimilation of Remote Sensing and WOFOST Model for Dynamically Monitoring Heavy Metal Stress in Rice. *IEEE J. Sel. Top. Appl. Earth Obs. Remote Sens.* **2016**, *9*, 1685–1695. [[CrossRef](#)]

43. Gaso, D.V.; Berger, A.G.; Ciganda, V.S. Predicting wheat grain yield and spatial variability at field scale using a simple regression or a crop model in conjunction with Landsat images. *Comput. Electron. Agric.* **2019**, *159*, 75–83. [[CrossRef](#)]
44. Beyene, A.N.; Zeng, H.; Wu, B.; Zhu, L.; Gebremicael, T.G.; Zhang, M.; Bezabh, T. Coupling remote sensing and crop growth model to estimate national wheat yield in Ethiopia. *Big Earth Data* **2021**, *6*, 18–35. [[CrossRef](#)]
45. Tripathy, R.; Chaudhari, K.N.; Mukherjee, J.; Ray, S.S.; Patel, N.K.; Panigrahy, S.; Parihar, J.S. Forecasting wheat yield in Punjab state of India by combining crop simulation model WOFOST and remotely sensed inputs. *Remote Sens. Lett.* **2013**, *4*, 19–28. [[CrossRef](#)]
46. Ji, F.; Meng, J.; Cheng, Z.; Fang, H.; Wang, Y. Crop Yield Estimation at Field Scales by Assimilating Time Series of Sentinel-2 Data Into a Modified CASA-WOFOST Coupled Model. *IEEE Trans. Geosci. Remote Sens.* **2021**, *60*, 1–14. [[CrossRef](#)]
47. Li, R.; Li, C.-J.; Dong, Y.-Y.; Liu, F.; Wang, J.-H.; Yang, X.-D.; Pan, Y.-C. Assimilation of Remote Sensing and Crop Model for LAI Estimation Based on Ensemble Kalman Filter. *Agric. Sci. China* **2011**, *10*, 1595–1602. [[CrossRef](#)]
48. Liu, Z.C.; Xu, Z.J.; Bi, R.; Wang, C.; He, P.; Jing, Y.D.; Yang, W.D. Estimation of Winter Wheat Yield in Arid and Semiarid Regions Based on Assimilated Multi-Source Sentinel Data and the CERES-Wheat Model. *Sensors* **2021**, *21*, 16. [[CrossRef](#)]
49. Liao, C.H.; Wang, J.F.; Dong, T.F.; Shang, J.L.; Liu, J.G.; Song, Y. Using spatio-temporal fusion of Landsat-8 and MODIS data to derive phenology, biomass and yield estimates for corn and soybean. *Sci. Total Environ.* **2019**, *650*, 1707–1721. [[CrossRef](#)]
50. Zhang, C.; Liu, J.; Dong, T.; Pattey, E.; Shang, J.; Tang, M.; Cai, H.; Saddique, Q. Coupling Hyperspectral Remote Sensing Data with a Crop Model to Study Winter Wheat Water Demand. *Remote Sens.* **2019**, *11*, 19. [[CrossRef](#)]
51. Casa, R.; Silvestro, P.C.; Yang, H.; Pignatti, S.; Pascucci, S.; Yang, G. Assimilation of remotely sensed canopy variables into crop models for an assessment of drought-related yield losses: A comparison of models of different complexity. In Proceedings of the 2016 IEEE International Geoscience and Remote Sensing Symposium (IGARSS), Beijing, China, 10–15 July 2016; IEEE: Piscataway, NJ, USA, 2016; pp. 5925–5928.
52. Jin, X.L.; Li, Z.H.; Feng, H.K.; Ren, Z.B.; Li, S.K. Estimation of maize yield by assimilating biomass and canopy cover derived from hyperspectral data into the AquaCrop model. *Agric. Water Manag.* **2020**, *227*, 10. [[CrossRef](#)]
53. Shi, L.; Hu, S.; Zha, Y. Estimation of Sugarcane Yield by Assimilating UAV and Ground Measurements Via Ensemble Kalman Filter. In Proceedings of the IGARSS 2018–2018 IEEE International Geoscience and Remote Sensing Symposium, Valencia, Spain, 22–27 July 2018; pp. 8816–8819. [[CrossRef](#)]
54. Yu, D.; Zha, Y.; Shi, L.; Jin, X.; Hu, S.; Yang, Q.; Huang, K.; Zeng, W. Improvement of sugarcane yield estimation by assimilating UAV-derived plant height observations. *Eur. J. Agron.* **2020**, *121*, 16. [[CrossRef](#)]
55. Jégo, G.; Pattey, E.; Liu, J. Using Leaf Area Index, retrieved from optical imagery, in the STICS crop model for predicting yield and biomass of field crops. *Field Crops Res.* **2012**, *131*, 63–74. [[CrossRef](#)]
56. Mohite, J.; Sawant, S.; Sakkan, M.; Shivalli, P.; Kodimela, K.; Pappula, S. Spatialization of rice crop yield using Sentinel-1 SAR and Oryza Crop Growth Simulation Model. In Proceedings of the 2019 8th International Conference on Agro-Geoinformatics (Agro-Geoinformatics), Istanbul, Turkey, 16–19 July 2019; pp. 1–6. [[CrossRef](#)]
57. Mokhtari, A.; Noory, H.; Vazifiedoust, M. Improving crop yield estimation by assimilating LAI and inputting satellite-based surface incoming solar radiation into SWAP model. *Agric. For. Meteorol.* **2018**, *250*, 159–170. [[CrossRef](#)]
58. Bai, T.C.; Wang, S.G.; Meng, W.B.; Zhang, N.N.; Wang, T.; Chen, Y.Q.; Mercatoris, B. Assimilation of Remotely-Sensed LAI into WOFOST Model with the SUBPLEX Algorithm for Improving the Field-Scale Jujube Yield Forecasts. *Remote Sens.* **2019**, *11*, 20. [[CrossRef](#)]
59. Bai, T.C.; Zhang, N.N.; Mercatoris, B.; Chen, Y.Q. Improving Jujube Fruit Tree Yield Estimation at the Field Scale by Assimilating a Single Landsat Remotely-Sensed LAI into the WOFOST Model. *Remote Sens.* **2019**, *11*, 22. [[CrossRef](#)]
60. Morel, J.; Martiné, J.; Bégué, A.; Todoroff, P.; Petit, M. A comparison of two coupling methods for improving a sugarcane model yield estimation with a NDVI-derived variable. *Proc. SPIE* **2012**, *8531*, 85310E. [[CrossRef](#)]
61. Ren, J.; Chen, Z.; Tang, H.; Yu, F.; Huang, Q. Simulation of regional winter wheat yield by combining epic model and remotely sensed LAI based on global optimization algorithm. In Proceedings of the 2011 IEEE International Geoscience and Remote Sensing Symposium, Vancouver, BC, Canada, 24–29 July 2011; pp. 4058–4061. [[CrossRef](#)]
62. Zhuo, W.; Huang, J.; Gao, X.; Ma, H.; Huang, H.; Su, W.; Meng, J.; Li, Y.; Chen, H.; Yin, D. Prediction of Winter Wheat Maturity Dates through Assimilating Remotely Sensed Leaf Area Index into Crop Growth Model. *Remote Sens.* **2020**, *12*, 19. [[CrossRef](#)]
63. Huang, J.; Ma, H.; Liu, J.; Zhu, D.; Zhang, X. Regional winter wheat yield estimation by assimilating MODIS ET and LAI products into SWAP model. In Proceedings of the 2013 Second International Conference on Agro-Geoinformatics (Agro-Geoinformatics), Fairfax, VA, USA, 12–16 August 2013; IEEE: Piscataway, NJ, USA, 2013; pp. 454–459.
64. Fahad, M.; Ahmad, I.; Rehman, M.; Waqas, M.M.; Gul, F. Regional Wheat Yield Estimation by Integration of Remotely Sensed Soil Moisture into a Crop Model. *Can. J. Remote Sens.* **2019**, *45*, 770–781. [[CrossRef](#)]
65. Tewes, A.; Hoffmann, H.; Nolte, M.; Krauss, G.; Schafer, F.; Kerkhoff, C.; Gaiser, T. How Do Methods Assimilating Sentinel-2-Derived LAI Combined with Two Different Sources of Soil Input Data Affect the Crop Model-Based Estimation of Wheat Biomass at Sub-Field Level? *Remote Sens.* **2020**, *12*, 21. [[CrossRef](#)]
66. Courault, D.; Hossard, L.; Demarez, V.; Dechatre, H.; Irfan, K.; Baghdadi, N.; Flamain, F.; Ruget, F. STICS crop model and Sentinel-2 images for monitoring rice growth and yield in the Camargue region. *Agron. Sustain. Dev.* **2021**, *41*, 49. [[CrossRef](#)]
67. Cheng, Z.Q.; Meng, J.H.; Wang, Y.M. Improving Spring Maize Yield Estimation at Field Scale by Assimilating Time-Series HJ-1 CCD Data into the WOFOST Model Using a New Method with Fast Algorithms. *Remote Sens.* **2016**, *8*, 22. [[CrossRef](#)]

68. Zhang, Z.; Li, Z.; Chen, Y.; Zhang, L.; Tao, F. Improving regional wheat yields estimations by multi-step-assimilating of a crop model with multi-source data. *Agric. For. Meteorol.* **2020**, *290*, 13. [[CrossRef](#)]
69. Machwitz, M.; Giustarini, L.; Bossung, C.; Frantz, D.; Schlerf, M.; Lilienthal, H.; Wandera, L.; Matgen, P.; Hoffmann, L.; Udelhoven, T. Enhanced biomass prediction by assimilating satellite data into a crop growth model. *Environ. Model. Softw.* **2014**, *62*, 437–453. [[CrossRef](#)]
70. Joshi, V.R.; Thorp, K.R.; Coulter, J.A.; Johnson, G.A.; Porter, P.M.; Strock, J.S.; Garcia, A.G.Y. Improving Site-Specific Maize Yield Estimation by Integrating Satellite Multispectral Data into a Crop Model. *Agronomy* **2019**, *9*, 18. [[CrossRef](#)]
71. Guo, C.L.; Tang, Y.N.; Lu, J.S.; Zhu, Y.; Cao, W.X.; Cheng, T.; Zhang, L.; Tian, Y.C. Predicting wheat productivity: Integrating time series of vegetation indices into crop modeling via sequential assimilation. *Agric. For. Meteorol.* **2019**, *272*, 69–80. [[CrossRef](#)]
72. Zhou, G.; Liu, M.; Liu, X.; Li, J. Combination of Crop Growth Model and Radiation Transfer Model with Remote Sensing Data Assimilation for Fapar Estimation. In Proceedings of the IGARSS 2018–2018 IEEE International Geoscience and Remote Sensing Symposium, Valencia, Spain, 22–27 July 2018; pp. 1882–1885. [[CrossRef](#)]
73. Betbeder, J.; Fieuzal, R.; Baup, F. Assimilation of LAI and Dry Biomass Data From Optical and SAR Images Into an Agro-Meteorological Model to Estimate Soybean Yield. *IEEE J. Top. Appl. Earth Obs. Remote Sens.* **2016**, *9*, 2540–2553. [[CrossRef](#)]
74. Zhang, T.; Su, J.; Liu, C.; Chen, W.-H. State and parameter estimation of the AquaCrop model for winter wheat using sensitivity informed particle filter. *Comput. Electron. Agric.* **2021**, *180*, 11. [[CrossRef](#)]
75. Dong, Y.Y.; Wang, J.H.; Li, C.J.; Yang, G.J.; Wang, Q.; Liu, F.; Zhao, J.L.; Wang, H.F.; Huang, W.J. Comparison and Analysis of Data Assimilation Algorithms for Predicting the Leaf Area Index of Crop Canopies. *IEEE J. Sel. Top. Appl. Earth Obs. Remote Sens.* **2013**, *6*, 188–201. [[CrossRef](#)]
76. Jin, X.L.; Kumar, L.; Li, Z.H.; Xu, X.G.; Yang, G.J.; Wang, J.H. Estimation of Winter Wheat Biomass and Yield by Combining the AquaCrop Model and Field Hyperspectral Data. *Remote Sens.* **2016**, *8*, 15. [[CrossRef](#)]
77. Liu, D.; Mishra, A.K.; Yu, Z.B. Evaluation of hydroclimatic variables for maize yield estimation using crop model and remotely sensed data assimilation. *Stoch. Environ. Res. Risk Assess.* **2019**, *33*, 1283–1295. [[CrossRef](#)]
78. Zhang, L.; Guo, C.L.; Zhao, L.Y.; Zhu, Y.; Cao, W.X.; Tian, Y.C.; Cheng, T.; Wang, X. Estimating wheat yield by integrating the WheatGrow and PROSAIL models. *Field Crops Res.* **2016**, *192*, 55–66. [[CrossRef](#)]
79. Guo, C.L.; Zhang, L.; Zhou, X.; Zhu, Y.; Cao, W.X.; Qiu, X.L.; Cheng, T.; Tian, Y.C. Integrating remote sensing information with crop model to monitor wheat growth and yield based on simulation zone partitioning. *Precis. Agric.* **2018**, *19*, 55–78. [[CrossRef](#)]
80. Huang, J.X.; Ma, H.Y.; Sedano, F.; Lewis, P.; Liang, S.; Wu, Q.L.; Su, W.; Zhang, X.D.; Zhu, D.H. Evaluation of regional estimates of winter wheat yield by assimilating three remotely sensed reflectance datasets into the coupled WOFOST-PROSAIL model. *Eur. J. Agron.* **2019**, *102*, 1–13. [[CrossRef](#)]
81. Li, Z.H.; Jin, X.L.; Zhao, C.J.; Wang, J.H.; Xu, X.G.; Yang, G.J.; Li, C.J.; Shen, J.X. Estimating wheat yield and quality by coupling the DSSAT-CERES model and proximal remote sensing. *Eur. J. Agron.* **2015**, *71*, 53–62. [[CrossRef](#)]
82. Pan, H.Z.; Chen, Z.X.; de Wit, A.; Ren, J.Q. Joint Assimilation of Leaf Area Index and Soil Moisture from Sentinel-1 and Sentinel-2 Data into the WOFOST Model for Winter Wheat Yield Estimation. *Sensors* **2019**, *19*, 17. [[CrossRef](#)]
83. Liu, Z.C.; Chao, W.; Bi, R.T.; Zhu, H.F.; He, P.; Jing, Y.D.; Yang, W.D. Winter wheat yield estimation based on assimilated Sentinel-2 images with the CERES-Wheat model. *J. Integr. Agric.* **2021**, *20*, 1958–1968. [[CrossRef](#)]
84. Silvestro, P.C.; Pignatti, S.; Pascucci, S.; Yang, H.; Li, Z.H.; Yang, G.J.; Huang, W.J.; Casa, R. Estimating Wheat Yield in China at the Field and District Scale from the Assimilation of Satellite Data into the Aquacrop and Simple Algorithm for Yield (SAFY) Models. *Remote Sens.* **2017**, *9*, 24. [[CrossRef](#)]
85. Li, Z.H.; Wang, J.H.; Xu, X.G.; Zhao, C.J.; Jin, X.L.; Yang, G.J.; Feng, H.K. Assimilation of Two Variables Derived from Hyperspectral Data into the DSSAT-CERES Model for Grain Yield and Quality Estimation. *Remote Sens.* **2015**, *7*, 12400–12418. [[CrossRef](#)]
86. Wang, H.; Zhu, Y.; Li, W.; Cao, W.; Tian, Y. Integrating remotely sensed leaf area index and leaf nitrogen accumulation with RiceGrow model based on particle swarm optimization algorithm for rice grain yield assessment. *J. Appl. Remote Sens.* **2014**, *8*, 16. [[CrossRef](#)]
87. Zhang, J.; Zhang, Z.; Wang, C.; Tao, F. Double-Rice System Simulation in a Topographically Diverse Region—A Remote-Sensing-Driven Case Study in Hunan Province of China. *Remote Sens.* **2019**, *11*, 19. [[CrossRef](#)]
88. Fang, H.; Liang, S.; Hoogenboom, G. Integration of MODIS LAI and vegetation index products with the CSM-CERES-Maize model for corn yield estimation. *Int. J. Remote Sens.* **2011**, *32*, 1039–1065. [[CrossRef](#)]
89. Manivasagam, V.S.; Sadeh, Y.; Kaplan, G.; Bonfil, D.J.; Rozenstein, O. Studying the Feasibility of Assimilating Sentinel-2 and PlanetScope Imagery into the SAFY Crop Model to Predict Within-Field Wheat Yield. *Remote Sens.* **2021**, *13*, 16. [[CrossRef](#)]
90. Zhang, C.; Liu, J.; Shang, J.; Dong, T.; Tang, M.; Feng, S.; Cai, H. Improving winter wheat biomass and evapotranspiration simulation by assimilating leaf area index from spectral information into a crop growth model. *Agric. Water Manag.* **2021**, *255*, 107057. [[CrossRef](#)]
91. Dong, T.F.; Liu, J.G.; Qian, B.D.; Zhao, T.; Jing, Q.; Geng, X.Y.; Wang, J.F.; Huffman, T.; Shang, J.L. Estimating winter wheat biomass by assimilating leaf area index derived from fusion of Landsat-8 and MODIS data. *Int. J. Appl. Earth Obs. Geoinf.* **2016**, *49*, 63–74. [[CrossRef](#)]
92. Son, N.; Chen, C.; Chen, C.; Chang, L.; Chiang, S. Rice yield estimation through assimilating satellite data into a crop simulation model. *Int. Arch. Photogramm. Remote Sens. Spat. Inf. Sci.* **2016**, *41*, 993–996. [[CrossRef](#)]

93. Jin, M.; Liu, X.N.; Wu, L.; Liu, M.L. An improved assimilation method with stress factors incorporated in the WOFOST model for the efficient assessment of heavy metal stress levels in rice. *Int. J. Appl. Earth Obs. Geoinf.* **2015**, *41*, 118–129. [[CrossRef](#)]
94. Mishra, V.; Cruise, J.F.; Mecikalski, J.R. Assimilation of coupled microwave/thermal infrared soil moisture profiles into a crop model for robust maize yield estimates over Southeast United States. *Eur. J. Agron.* **2021**, *123*, 15. [[CrossRef](#)]
95. Cheng, Z.Q.; Meng, J.H.; Shang, J.L.; Liu, J.G.; Qiao, Y.Y.; Qian, B.D.; Jing, Q.; Dong, T.F. Improving Soil Available Nutrient Estimation by Integrating Modified WOFOST Model and Time-Series Earth Observations. *IEEE Trans. Geosci. Remote Sens.* **2019**, *57*, 2896–2908. [[CrossRef](#)]
96. De Wit, A.; Duveiller, G.; Defourny, P. Estimating regional winter wheat yield with WOFOST through the assimilation of green area index retrieved from MODIS observations. *Agric. For. Meteorol.* **2012**, *164*, 39–52. [[CrossRef](#)]
97. Wu, S.; Yang, P.; Ren, J.; Chen, Z.; Li, H. Regional winter wheat yield estimation based on the WOFOST model and a novel VW-4DnSRF assimilation algorithm. *Remote Sens. Environ.* **2021**, *255*, 22. [[CrossRef](#)]
98. Xu, W.; Jiang, H.; Huang, J. Regional Crop Yield Assessment by Combination of a Crop Growth Model and Phenology Information Derived from MODIS. *Sens. Lett.* **2011**, *9*, 981–989. [[CrossRef](#)]
99. Pagani, V.; Guarneri, T.; Busetto, L.; Ranghetti, L.; Boschetti, M.; Movedi, E.; Campos-Taberner, M.; Javier Garcia-Haro, F.; Katsantonis, D.; Stavrakoudis, D.; et al. A high-resolution, integrated system for rice yield forecasting at district level. *Agric. Syst.* **2019**, *168*, 181–190. [[CrossRef](#)]
100. Zhu, X.; Zhao, Y.; Feng, X. A methodology for estimating Leaf Area Index by assimilating remote sensing data into crop model based on temporal and spatial knowledge. *Chin. Geogr. Sci.* **2013**, *23*, 550–561. [[CrossRef](#)]
101. Shawon, A.R.; Ko, J.; Ha, B.; Jeong, S.; Kim, D.K.; Kim, H.Y. Assessment of a Proximal Sensing-integrated Crop Model for Simulation of Soybean Growth and Yield. *Remote Sens.* **2020**, *12*, 22. [[CrossRef](#)]
102. Jiang, Z.W.; Chen, Z.X.; Chen, J.; Liu, J.; Ren, J.Q.; Li, Z.N.; Sun, L.; Li, H. Application of Crop Model Data Assimilation With a Particle Filter for Estimating Regional Winter Wheat Yields. *IEEE J. Sel. Top. Appl. Earth Obs. Remote Sens.* **2014**, *7*, 4422–4431. [[CrossRef](#)]
103. Li, Y.; Zhou, Q.G.; Zhou, J.; Zhang, G.F.; Chen, C.; Wang, J. Assimilating remote sensing information into a coupled hydrology-crop growth model to estimate regional maize yield in arid regions. *Ecol. Model.* **2014**, *291*, 15–27. [[CrossRef](#)]
104. Dong, Y.Y.; Zhao, C.J.; Yang, G.J.; Chen, L.P.; Wang, J.H.; Feng, H.K. Integrating a very fast simulated annealing optimization algorithm for crop leaf area index variational assimilation. *Math. Comput. Model.* **2013**, *58*, 871–879. [[CrossRef](#)]
105. Jogo, G.; Pattey, E.; Mesbah, S.M.; Liu, J.G.; Duchesne, I. Impact of the spatial resolution of climatic data and soil physical properties on regional corn yield predictions using the STICS crop model. *Int. J. Appl. Earth Obs. Geoinf.* **2015**, *41*, 11–22. [[CrossRef](#)]
106. Nguyen, V.; Jeong, S.; Ko, J.; Ng, C.T.; Yeom, J. Mathematical Integration of Remotely-Sensed Information into a Crop Modelling Process for Mapping Crop Productivity. *Remote Sens.* **2019**, *11*, 17. [[CrossRef](#)]
107. El Sharif, H.; Wang, J.F.; Georgakakos, A.P. Modeling Regional Crop Yield and Irrigation Demand Using SMAP Type of Soil Moisture Data. *J. Hydrometeorol.* **2015**, *16*, 904–916. [[CrossRef](#)]
108. Mabhaudhi, T.; Modi, A.T. Indigenous crops: Sowing the seeds of knowledge on underutilised crops. *Water Wheel* **2016**, *15*, 40–41.
109. Wimalasiri, E.M.; Jahanshiri, E.; Chimonyo, V.; Azam-Ali, S.N.; Gregory, P.J. Crop model ideotyping for agricultural diversification. *MethodsX* **2021**, *8*, 101420. [[CrossRef](#)]
110. Chen, Y.; Zhang, Z.; Tao, F.L. Improving regional winter wheat yield estimation through assimilation of phenology and leaf area index from remote sensing data. *Eur. J. Agron.* **2018**, *101*, 163–173. [[CrossRef](#)]
111. Novelli, F.; Vuolo, F. Assimilation of Sentinel-2 Leaf Area Index Data into a Physically-Based Crop Growth Model for Yield Estimation. *Agronomy* **2019**, *9*, 18. [[CrossRef](#)]
112. Jiang, J.; Johansen, K.; Tu, Y.-H.; McCabe, M.F. Multi-sensor and multi-platform consistency and interoperability between UAV, Planet CubeSat, Sentinel-2, and Landsat reflectance data. *GIScience Remote Sens.* **2022**, *59*, 936–958. [[CrossRef](#)]
113. Cheng, Z.Q.; Meng, J.H.; Shang, J.L.; Liu, J.G.; Huang, J.X.; Qiao, Y.Y.; Qian, B.D.; Jing, Q.; Dong, T.F.; Yu, L.H. Generating Time-Series LAI Estimates of Maize Using Combined Methods Based on Multispectral UAV Observations and WOFOST Model. *Sensors* **2020**, *20*, 19. [[CrossRef](#)]
114. Nhamo, L.; Magidi, J.; Nyamugama, A.; Clulow, A.D.; Sibanda, M.; Chimonyo, V.G.; Mabhaudhi, T. Prospects of improving agricultural and water productivity through unmanned aerial vehicles. *Agriculture* **2020**, *10*, 256. [[CrossRef](#)]
115. Jin, X.L.; Li, Z.H.; Yang, G.J.; Yang, H.; Feng, H.K.; Xu, X.G.; Wang, J.H.; Li, X.C.; Luo, J.H. Winter wheat yield estimation based on multi-source medium resolution optical and radar imaging data and the AquaCrop model using the particle swarm optimization algorithm. *ISPRS J. Photogramm. Remote Sens.* **2017**, *126*, 24–37. [[CrossRef](#)]
116. Maki, M.; Sekiguchi, K.; Homma, K.; Hirooka, Y.; Oki, K. Estimation of rice yield by SIMRIW-RS, a model that integrates remote sensing data into a crop growth model. *J. Agric. Meteorol.* **2017**, *73*, 2–8. [[CrossRef](#)]
117. Wu, S.; Yang, P.; Chen, Z.; Ren, J.; Li, H.; Sun, L. Estimating winter wheat yield by assimilation of remote sensing data with a four-dimensional variation algorithm considering anisotropic background error and time window. *Agric. For. Meteorol.* **2021**, *301–302*, 16. [[CrossRef](#)]
118. Chen, P.F. Estimation of Winter Wheat Grain Protein Content Based on Multisource Data Assimilation. *Remote Sens.* **2020**, *12*, 20. [[CrossRef](#)]

119. Casa, R.; Silvestro, P.C.; Yang, H.; Pignatti, S.; Pascucci, S.; Yang, G. Development of farmland drought assessment tools based on the assimilation of remotely sensed canopy biophysical variables into crop water response models. In Proceedings of the 2015 IEEE International Geoscience and Remote Sensing Symposium (IGARSS), Milan, Italy, 26–31 July 2015; IEEE: Piscataway, NJ, USA, 2015; pp. 4005–4008.
120. Thorp, K.R.; Wang, G.; West, A.L.; Moran, M.S.; Bronson, K.F.; White, J.W.; Mon, J. Estimating crop biophysical properties from remote sensing data by inverting linked radiative transfer and ecophysiological models. *Remote Sens. Environ.* **2012**, *124*, 224–233. [[CrossRef](#)]
121. Hank, T.B.; Bach, H.; Mauser, W. Using a Remote Sensing-Supported Hydro-Agroecological Model for Field-Scale Simulation of Heterogeneous Crop Growth and Yield: Application for Wheat in Central Europe. *Remote Sens.* **2015**, *7*, 3934–3965. [[CrossRef](#)]
122. Jindo, K.; Kozan, O.; de Wit, A. Data Assimilation of Remote Sensing Data into a Crop Growth Model. In *Precision Agriculture: Modelling*; Springer: Berlin/Heidelberg, Germany, 2023; pp. 185–197.
123. Ma, G.N.; Huang, J.X.; Wu, W.B.; Fan, J.L.; Zou, J.Q.; Wu, S.J. Assimilation of MODIS-LAI into the WOFOST model for forecasting regional winter wheat yield. *Math. Comput. Model.* **2013**, *58*, 634–643. [[CrossRef](#)]
124. Li, H.; Chen, Z.X.; Liu, G.H.; Jiang, Z.W.; Huang, C. Improving Winter Wheat Yield Estimation from the CERES-Wheat Model to Assimilate Leaf Area Index with Different Assimilation Methods and Spatio-Temporal Scales. *Remote Sens.* **2017**, *9*, 23. [[CrossRef](#)]
125. Du, L.; Xu, L.; Li, Y.; Liu, C.; Li, Z.; Wong, J.S.; Lei, B. China's Agricultural Irrigation and Water Conservancy Projects: A Policy Synthesis and Discussion of Emerging Issues. *Sustainability* **2019**, *11*, 7027. [[CrossRef](#)]
126. Bai, Y.; Wong, M.; Shi, W.-Z.; Wu, L.-X.; Qin, K. Advancing of Land Surface Temperature Retrieval Using Extreme Learning Machine and Spatio-Temporal Adaptive Data Fusion Algorithm. *Remote Sens.* **2015**, *7*, 4424–4441. [[CrossRef](#)]
127. Cucho-Padin, G.; Loayza, H.; Palacios, S.; Balcazar, M.; Carbajal, M.; Quiroz, R. Development of low-cost remote sensing tools and methods for supporting smallholder agriculture. *Appl. Geomat.* **2019**, *12*, 247–263. [[CrossRef](#)]
128. Antle, J.M.; Valdivia, R.O.; Boote, K.J.; Janssen, S.; Jones, J.W.; Porter, C.H.; Rosenzweig, C.; Ruane, A.C.; Thorburn, P.J. AgMIP's transdisciplinary agricultural systems approach to regional integrated assessment of climate impacts, vulnerability, and adaptation. In *Handbook of Climate Change and Agroecosystems*; Imperial College Press: London, UK, 2015; pp. 27–44.
129. Gitz, V.; Meybeck, A.; Lipper, L.; Young, C.D.; Braatz, S. Climate change and food security: Risks and responses. *Food Agric. Organ. United Nations (FAO) Rep.* **2016**, *110*, 2–4.
130. Zinyengere, N.; Crespo, O.; Hachigonta, S.; Tadross, M.-U.N.D.P. Crop model usefulness in drylands of southern Africa: An application of DSSAT. *South Afr. J. Plant Soil* **2015**, *32*, 95–104. [[CrossRef](#)]
131. Leroux, L.; Baron, C.; Zougrana, B.; Traore, S.B.; Lo Seen, D.; Begue, A. Crop Monitoring Using Vegetation and Thermal Indices for Yield Estimates: Case Study of a Rainfed Cereal in Semi-Arid West Africa. *IEEE J. Sel. Top. Appl. Earth Obs. Remote Sens.* **2016**, *9*, 347–362. [[CrossRef](#)]
132. Chivasa, W.; Mutanga, O.; Biradar, C. Application of remote sensing in estimating maize grain yield in heterogeneous African agricultural landscapes: A review. *Int. J. Remote Sens.* **2017**, *38*, 6816–6845. [[CrossRef](#)]
133. Zinyengere, N.; Crespo, O.; Hachigonta, S.; Tadross, M. Local impacts of climate change and agronomic practices on dry land crops in Southern Africa. *Agric. Ecosyst. Environ.* **2014**, *197*, 1–10. [[CrossRef](#)]
134. Rurinda, J.; van Wijk, M.T.; Mapfumo, P.; Descheemaeker, K.; Supit, I.; Giller, K.E. Climate change and maize yield in southern Africa: What can farm management do? *Glob. Chang. Biol.* **2015**, *21*, 4588–4601. [[CrossRef](#)]
135. Blatchford, M.L.; Mannaerts, C.M.; Njuki, S.M.; Nouri, H.; Zeng, Y.; Pelgrum, H.; Wonink, S.; Karimi, P. Evaluation of WaPOR V2 evapotranspiration products across Africa. *Hydrol. Process.* **2020**, *34*, 3200–3221. [[CrossRef](#)]
136. Gilardelli, C.; Stella, T.; Confalonieri, R.; Ranghetti, L.; Campos-Taberner, M.; Garcia-Haro, F.J.; Boschetti, M. Downscaling rice yield simulation at sub-field scale using remotely sensed LAI data. *Eur. J. Agron.* **2019**, *103*, 108–116. [[CrossRef](#)]
137. Gao, X.; Huang, J.; Ma, H.; Zhuo, W.; Zhu, D. Regional winter wheat maturity date prediction using remote sensing-crop model data assimilation and numerical weather prediction. In Proceedings of the 2018 7th International Conference on Agro-geoinformatics (Agro-geoinformatics), Hangzhou, China, 6–9 August 2018; IEEE: Piscataway, NJ, USA, 2018; pp. 1–5.
138. Jeong, S.; Ko, J.; Kang, M.; Yeom, J.; Ng, C.T.; Lee, S.H.; Lee, Y.G.; Kim, H.Y. Geographical variations in gross primary production and evapotranspiration of paddy rice in the Korean Peninsula. *Sci. Total Environ.* **2020**, *714*, 23. [[CrossRef](#)] [[PubMed](#)]
139. Jeong, S.; Ko, J.; Yeom, J.-M. Nationwide Projection of Rice Yield Using a Crop Model Integrated with Geostationary Satellite Imagery: A Case Study in South Korea. *Remote Sens.* **2018**, *10*, 1665. [[CrossRef](#)]
140. Wagner, M.P.; Slawig, T.; Taravat, A.; Oppelt, N. Remote Sensing Data Assimilation in Dynamic Crop Models Using Particle Swarm Optimization. *ISPRS Int. Geo-Inf.* **2020**, *9*, 24. [[CrossRef](#)]
141. Zhao, B.; Liu, M.; Wu, J.; Liu, X.; Liu, M.; Wu, L. Parallel Computing for Obtaining Regional Scale Rice Growth Conditions Based on WOFOST and Satellite Images. *IEEE Access* **2020**, *8*, 223675–223685. [[CrossRef](#)]
142. Zhao, H.; Pei, Z. Crop growth monitoring by integration of time series remote sensing imagery and the WOFOST model. In Proceedings of the 2013 Second International Conference on Agro-Geoinformatics (Agro-Geoinformatics), Fairfax, VA, USA, 12–16 August 2013; pp. 568–571. [[CrossRef](#)]
143. Zhou, H.; Wu, J.; Li, X.; Geng, G.; Liu, L. Improving soil moisture estimation by assimilating remotely sensed data into crop growth model for agricultural drought monitoring. In Proceedings of the 2016 IEEE International Geoscience and Remote Sensing Symposium (IGARSS), Beijing, China, 10–15 July 2016; pp. 4229–4232. [[CrossRef](#)]

144. Jin, H.A.; Li, A.N.; Wang, J.D.; Bo, Y.C. Improvement of spatially and temporally continuous crop leaf area index by integration of CERES-Maize model and MODIS data. *Eur. J. Agron.* **2016**, *78*, 1–12. [[CrossRef](#)]
145. Huang, J.X.; Tian, L.Y.; Liang, S.L.; Ma, H.Y.; Becker-Reshef, I.; Huang, Y.B.; Su, W.; Zhang, X.D.; Zhu, D.H.; Wu, W.B. Improving winter wheat yield estimation by assimilation of the leaf area index from Landsat TM and MODIS data into the WOFOST model. *Agric. For. Meteorol.* **2015**, *204*, 106–121. [[CrossRef](#)]
146. Cheng, Z.Q.; Meng, J.H.; Qiao, Y.Y.; Wang, Y.M.; Dong, W.Q.; Han, Y.X. Preliminary Study of Soil Available Nutrient Simulation Using a Modified WOFOST Model and Time-Series Remote Sensing Observations. *Remote Sens.* **2018**, *10*, 21. [[CrossRef](#)]
147. Huang, H.; Huang, J.; Wu, Y. Markov Chain Monte Carlo and Four-Dimensional Variational Approach Based Winter Wheat Yield Estimation. In Proceedings of the IGARSS 2020-2020 IEEE International Geoscience and Remote Sensing Symposium, Waikoloa, HI, USA, 26 September–2 October 2020; pp. 5290–5293. [[CrossRef](#)]
148. Huang, Y.; Zhu, Y.; Li, W.; Cao, W.; Tian, Y. Assimilating Remotely Sensed Information with the WheatGrow Model Based on the Ensemble Square Root Filter for Improving Regional Wheat Yield Forecasts. *Plant. Prod. Sci.* **2013**, *16*, 352–364. [[CrossRef](#)]
149. Jiang, Z.W.; Chen, Z.X.; Chen, J.; Ren, J.Q.; Li, Z.N.; Sun, L. The Estimation of Regional Crop Yield Using Ensemble-Based Four-Dimensional Variational Data Assimilation. *Remote Sens.* **2014**, *6*, 2664–2681. [[CrossRef](#)]
150. Li, H.; Jiang, Z.W.; Chen, Z.X.; Ren, J.Q.; Liu, B.; Hasituyu. Assimilation of temporal-spatial leaf area index into the CERES-Wheat model with ensemble Kalman filter and uncertainty assessment for improving winter wheat yield estimation. *J. Integr. Agric.* **2017**, *16*, 2283–2299. [[CrossRef](#)]
151. Liu, P.W.; Bongiovanni, T.; Monsivais-Huertero, A.; Judge, J.; Steele-Dunne, S.; Bindlish, R.; Jackson, T.J. Assimilation of Active and Passive Microwave Observations for Improved Estimates of Soil Moisture and Crop Growth. *IEEE J. Sel. Top. Appl. Earth Obs. Remote Sens.* **2016**, *9*, 1357–1369. [[CrossRef](#)]
152. Ma, H.; Huang, J.; Zhu, D.; Liu, J.; Su, W.; Zhang, C.; Fan, J. Estimating regional winter wheat yield by assimilation of time series of HJ-1 CCD NDVI into WOFOST-ACRM model with Ensemble Kalman Filter. *Math. Comput. Model.* **2013**, *58*, 759–770. [[CrossRef](#)]
153. Wang, J.; Li, X.; Lu, L.; Fang, F. Estimating near future regional corn yields by integrating multi-source observations into a crop growth model. *Eur. J. Agron.* **2013**, *49*, 126–140. [[CrossRef](#)]
154. Wang, X.; Jia, K.; Liang, S.; Zhang, Y. Fractional Vegetation Cover Estimation Method Through Dynamic Bayesian Network Combining Radiative Transfer Model and Crop Growth Model. *IEEE Trans. Geosci. Remote Sens.* **2016**, *54*, 7442–7450. [[CrossRef](#)]
155. Wang, L.; Huang, J.; Wang, L.; Huang, J.; Wang, L.; Huang, J.; Gao, P.; Wu, H. Estimating winter wheat yield by assimilation of MODIS LAI into WOFOST model with Ensemble Kalman Filter. In Proceedings of the 2017 6th International Conference on Agro-Geoinformatics, Fairfax VA, USA, 7–10 August 2017; pp. 1–5. [[CrossRef](#)]
156. Wu, S.; Huang, J.; Liu, X.; Fan, J.; Ma, G.; Zou, J. Assimilating MODIS-LAI into Crop Growth Model with EnKF to Predict Regional Crop Yield. In *Computer and Computing Technologies in Agriculture V*; Li, D., Chen, Y., Eds.; Springer: Berlin/Heidelberg, Germany, 2012; pp. 410–418.
157. Zhuo, W.; Huang, J.; Li, L.; Zhang, X.; Ma, H.; Gao, X.; Huang, H.; Xu, B.; Xiao, X. Assimilating Soil Moisture Retrieved from Sentinel-1 and Sentinel-2 Data into WOFOST Model to Improve Winter Wheat Yield Estimation. *Remote Sens.* **2019**, *11*, 17. [[CrossRef](#)]

Disclaimer/Publisher’s Note: The statements, opinions and data contained in all publications are solely those of the individual author(s) and contributor(s) and not of MDPI and/or the editor(s). MDPI and/or the editor(s) disclaim responsibility for any injury to people or property resulting from any ideas, methods, instructions or products referred to in the content.